De novo assembly of a PML nuclear subcompartment occurs through multiple pathways and induces telomere elongation

Inn Chung[1], Heinrich Leonhardt[2] and Karsten Rippe[1,*]

[1]German Cancer Research Center & BioQuant, Research Group Genome Organization & Function, Im Neuenheimer Feld 280, 69120 Heidelberg, Germany
[2]Department of Biology II, Center for Integrated Protein Science, Ludwig Maximilians University Munich, 82152 Planegg-Martinsried, Germany
*Author for correspondence (Karsten.Rippe@dkfz.de)

Accepted 10 June 2011
Journal of Cell Science 124, 3603–3618

doi: 10.1242/jcs.084681

Summary

Telomerase-negative tumor cells use an alternative lengthening of telomeres (ALT) pathway that involves DNA recombination and repair to maintain their proliferative potential. The cytological hallmark of this process is the accumulation of promyelocytic leukemia (PML) nuclear protein at telomeric DNA to form ALT-associated PML bodies (APBs). Here, the de novo formation of a telomeric PML nuclear subcompartment was investigated by recruiting APB protein components. We show that functionally distinct proteins were able to initiate the formation of bona fide APBs with high efficiency in a self-organizing and self-propagating manner. These included: (1) PML and Sp100 as the constituting components of PML nuclear bodies, (2) telomere repeat binding factors 1 and 2 (TRF1 and TRF2, respectively), (3) the DNA repair protein NBS1 and (4) the SUMO E3 ligase MMS21, as well as the isolated SUMO1 domain, through an interacting domain of another protein factor. By contrast, the repair factors Rad9, Rad17 and Rad51 were less efficient in APB nucleation but were recruited to preassembled APBs. The artificially created APBs induced telomeric extension through a DNA repair mechanism, as inferred from their colocalization with sites of non-replicative DNA synthesis and histone H2A.X phosphorylation, and an increase of the telomere repeat length. These activities were absent after recruitment of the APB factors to a pericentric locus and establish APBs as functional intermediates of the ALT pathway.

Key words: Alternative lengthening of telomeres, DNA repair, DNA recombination, Promyelocytic leukemia nuclear bodies

Introduction

Telomeres, the ends of the linear chromosomes, contain repetitive DNA sequences [in humans $(TTAGGG)_n$, typically 3–20 kb in length] that are organized into a specialized nucleoprotein complex. This structure protects the telomeres from being processed as a DNA double-strand break (DSB) by the DNA repair and recombination machinery of the cell (de Lange et al., 2006; Verdun and Karlseder, 2007). Telomeres shorten with every cell division owing to the incomplete replication of the lagging strand and additional exonucleolytic activities. Upon reaching a critical length cellular senescence is induced (Collado et al., 2007). In most tumor cells the reverse transcriptase telomerase is reactivated and the telomere repeat sequences can be extended, thereby allowing unlimited proliferation. However, some immortalized cell lines and 10–15% of cancer cells use an alternative lengthening of telomeres (ALT) mechanism for the maintenance of their telomere repeats (Henson et al., 2002). This pathway involves DNA repair and recombination processes (Dunham et al., 2000). ALT-positive cells are characterized by the association of telomeric DNA with promyelocytic leukemia nuclear bodies (PML-NBs), forming ALT-associated PML-NBs (APBs) (Henson et al., 2002). PML-NBs are mobile nuclear subcompartments present in most mammalian cells and have been implicated in a variety of cellular functions including apoptosis, senescence, tumor suppression, transcription, antiviral response and DNA replication and repair (Bernardi and Pandolfi, 2007; Dellaire and Bazett-Jones, 2004; Lallemand-Breitenbach and de The, 2010; Takahashi et al., 2004). APBs colocalize with DNA repair and recombination proteins, and a number of models for the molecular mechanisms have been proposed to explain the role of APBs in the ALT pathway (Cesare and Reddel, 2010; Draskovic et al., 2009; Henson et al., 2002; Jiang et al., 2007). However, it is not clear whether a functional link between APB formation and telomere lengthening exists. To address this issue, we investigated the de novo formation of APBs. Protein components of APBs were recruited to telomeres tagged with stable integrations of bacterial *lac* operator DNA sequence (*lac*O) repeats in the ALT-positive human osteosarcoma U2OS cell line (Jegou et al., 2009). This system allowed elucidating the APB assembly process after enriching one factor and the dissection of the interaction network that leads to APB formation and the recruitment of DNA repair and recombination factors. Furthermore, we show that the de novo formation of APBs induced the elongation of telomeric repeats in a DNA repair based synthesis process. These results demonstrate that APBs are indeed functional intermediates in the ALT pathway and identify them as potential targets for the treatment of ALT-positive tumors.

Results

Recruitment of PML and Sp100 to *lac*O-labeled telomeres leads to the de novo assembly of bona fide APBs

The ALT-positive U2OS cell line F6B2, which has three stable integrations of bacterial *lac* operator (*lac*O) repeats (referred to as

telomeric *lac*O arrays) directly adjacent to the telomeres of chromosomes 6q, 11p and 12q (Jegou et al., 2009), was transfected with a bacterial LacI repressor fused to a GFP-binding protein (GBP) (Rothbauer et al., 2006; Zolghadr et al., 2008). The LacI construct with (GBP–LacI–RFP) or without (GBP–LacI) an additional red fluorescent mRFP1 marker was used to recruit GFP- or YFP-tagged proteins and interacting factors to the telomere-associated *lac*O arrays (Fig. 1A). As described in previous studies, the GBP domain binds with high affinity to GFP with an equilibrium dissociation constant of 0.23 nM (Rothbauer et al., 2006). Thus, this system is equivalent to the use of direct fusion constructs of LacI with the protein of interest (Kaiser et al., 2008; Soutoglou and Misteli, 2008; Tumbar et al., 1999). Accordingly, the recruitment of GFP–PML through GBP–LacI–RFP in the F6B2 cell line resulted in colocalization of GFP–PML with three telomeres (Fig. 1B). In order to address whether tethering PML to the *lac*O-labeled telomeres leads to the assembly of APB-like structures at these sites, the presence of the main structural components of PML-NBs was analyzed. For this, we used the PML III splicing variant that itself appears to have no specific interactions with shelterin proteins (e.g. TRF1 and TRF2), as opposed to PML IV (corresponding to PML 3 in the arabic numbering scheme) for which binding to TRF1 has been reported (Yu et al., 2009). Whereas PML IV showed a behavior similar to that of PML III in control experiments (data not shown), the use of PML III allowed us to separate the initial telomeric recruitment event (provided in our system by *lac*O and GBP–LacI) more clearly from the other protein–protein interactions of PML.

PML-NBs are composed of PML and Sp100 proteins that carry post-translational small ubiquitin-like modifier (SUMO) modifications and organize in a spherical shell (Bernardi and Pandolfi, 2007; Lang et al., 2010; Shen et al., 2006). Accordingly, we investigated whether PML or Sp100 recruitment would result in the accumulation of other components (Fig. 2). GFP-tagged PML protein was efficiently bound to the *lac*O arrays through GBP–LacI–RFP. This triggered the subsequent recruitment of endogenous Sp100 to these sites with an efficiency of 100% (Fig. 2A). The reverse experiment, tethering GFP–Sp100 to the *lac*O arrays, also induced the formation of PML-NBs because endogenous PML was detected at all GFP–Sp100-positive telomeric *lac*O arrays (Fig. 2B). Furthermore, the recruitment of GFP–PML increased the presence of endogenous SUMO isoforms to more than 90% ($93\pm9\%$ for SUMO1, $98\pm11\%$ for SUMO2 and SUMO3, Fig. 2C,D). By contrast, transfection of only GBP–LacI–RFP or GBP–LacI–RFP together with the isolated GFP domain did not lead to a significant enrichment of endogenous PML or Sp100 at these sites (Fig. 2E; supplementary material Fig. S1A). Likewise, co-transfecting RFP–LacI without the GBP domain together with GFP–PML did not target PML to the *lac*O arrays (data not shown). The residual degree of colocalization in the control cells is likely to reflect the presence of endogenously formed APBs at the three tagged telomeres, as well as random superposition of the two signals in the same optical section of the confocal images.

The analysis of the de-novo-assembled APB-like structures by confocal laser scanning microscopy (CLSM) revealed a cap-like organization of PML protein around telomeric repeats (Fig. 1B; supplementary material Fig. S1) that was indistinguishable from that

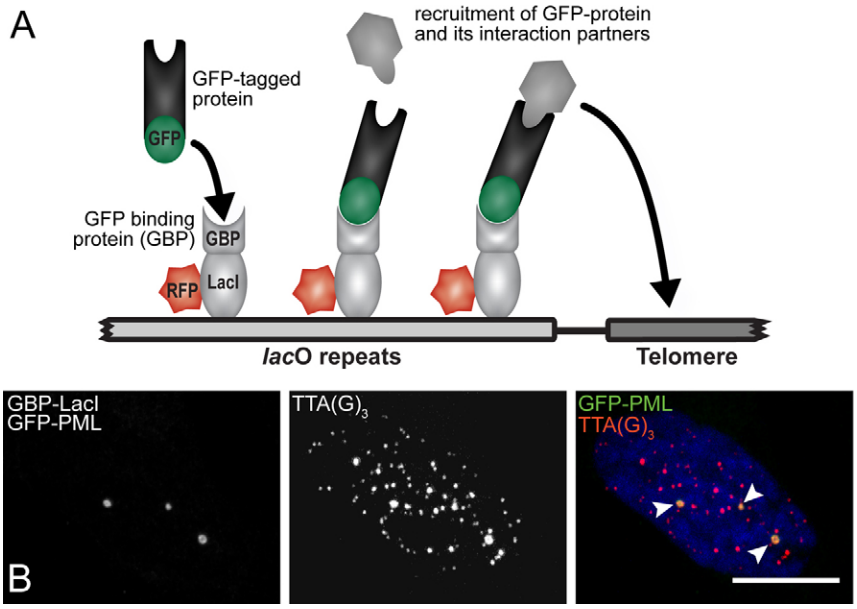

Fig. 1. Experimental approach for studying de-novo-formed complexes of PML nuclear bodies (APBs) at the telomeres. (**A**) Schematic representation of the experimental approach. The U2OS cell clone F6B2 employed in this study has three integration sites of the *lac*O arrays, adjacent to the telomeres of chromosomes 6q, 11p and 12q (Jegou et al., 2009). Different GFP-tagged proteins were recruited to the *lac*O arrays through a fusion of LacI repressor to a high-affinity GFP-binding domain (GBP) and a red fluorescent protein domain (GBP–LacI–RFP). Endogenous interaction partners of the GFP-labeled protein were then identified by subsequent immunostaining and evaluation of the colocalization of the fluorescence signals by confocal laser scanning microscopy (Rothbauer et al., 2006; Zolghadr et al., 2008). (**B**) The F6B2 U2OS cell line was co-transfected with GFP–PML and GBP–LacI expression vectors. Through binding of GBP–LacI to the *lac*O repeat sequences, GFP–PML was recruited to these sites. Staining of the telomeric repeats $TTA(G)_3$ with a Cy3-labeled PNA probe revealed the colocalization of telomeres with the GFP–PML signal in the confocal images (see arrows). This indicates the formation of bona fide APBs at the three telomere sites of chromosomes 6q, 11p and 12q. Scale bar: 10 μm.

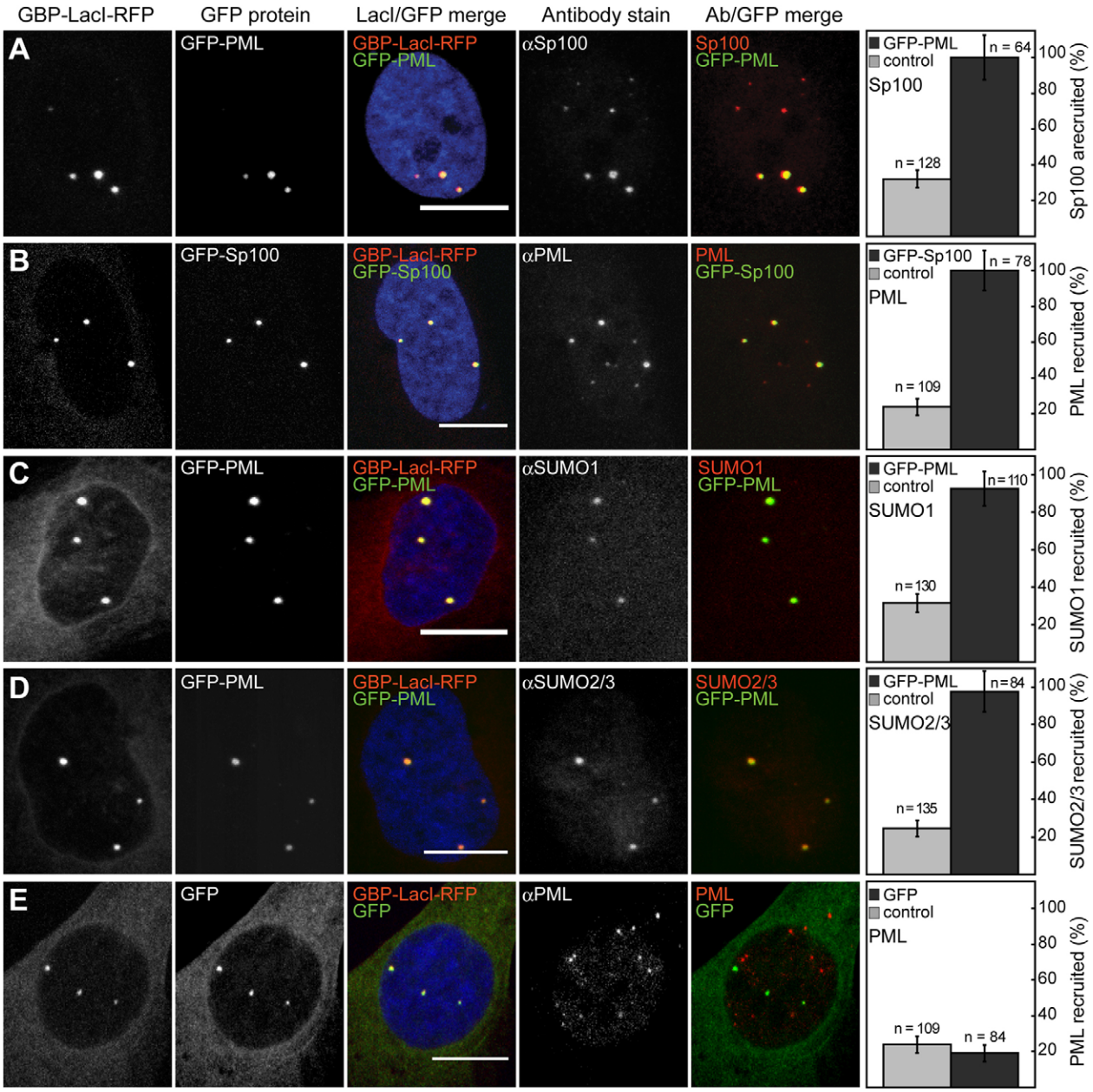

Fig. 2. Formation of a de novo APB by recruitment of PML and Sp100 protein. Cells were co-transfected with GBP–LacI–RFP and the indicated GFP constructs. This resulted in the tethering of the GFP-tagged protein to the three *lac*O-labeled telomeres. Association of the main APB components, PML, Sp100 and SUMO, was detected by immunostaining the endogenous proteins and evaluating the colocalization of the two fluorescence signals in optical sections obtained by confocal laser scanning microscopy imaging. (**A**) Recruitment of GFP–PML yielded 100% colocalization with endogenous Sp100 compared with 24±5% in the absence of GFP–PML ($P<0.0001$). (**B**) GFP–Sp100 displayed 100% colocalization with endogenous PML compared with the control value of 32±5% in the absence of GFP–Sp100 ($P<0.0001$). (**C**,**D**) GFP–PML induced 93±9% (endogenous SUMO1) and 98±11% [endogenous SUMO2 and SUMO3 (SUMO2/3)] colocalization compared with 32±5% and 24±4% in the control experiments, in which GFP–PML was absent ($P<0.0001$ for both analyses). (**E**) Recruitment of the isolated GFP domain. This led to a colocalization of only 19±5% with endogenous PML, which did not significantly differ from the 20–30% background observed in the control transfection with only GBP–LacI–RFP ($P=0.48$). Scale bars: 10 µm. All error bars show the s.d.

of endogenous APBs (Jegou et al., 2009; Lang et al., 2010). Two telomere signals within one APB could only be distinguished in a very small fraction (0.3±0.1%) of the de-novo-formed telomeric PML subcompartments evaluated here. For endogenous APBs in U2OS cells this number was even lower at ~0.10±0.04% (six out of 5803). These results were obtained with an advanced automated three-dimensional image analysis of confocal three-dimensional stacks of endogenous APBs in U2OS cells visualized by immunostaining against PML and TRF2 using the method described previously (Osterwald et al., 2011; Wörz et al., 2010).

Together, our results indicate that the artificial enrichment of GFP–PML at *lac*O-tagged telomeres led to the assembly of bona fide APBs (defined as PML-NBs at telomeres) with respect to their structural composition.

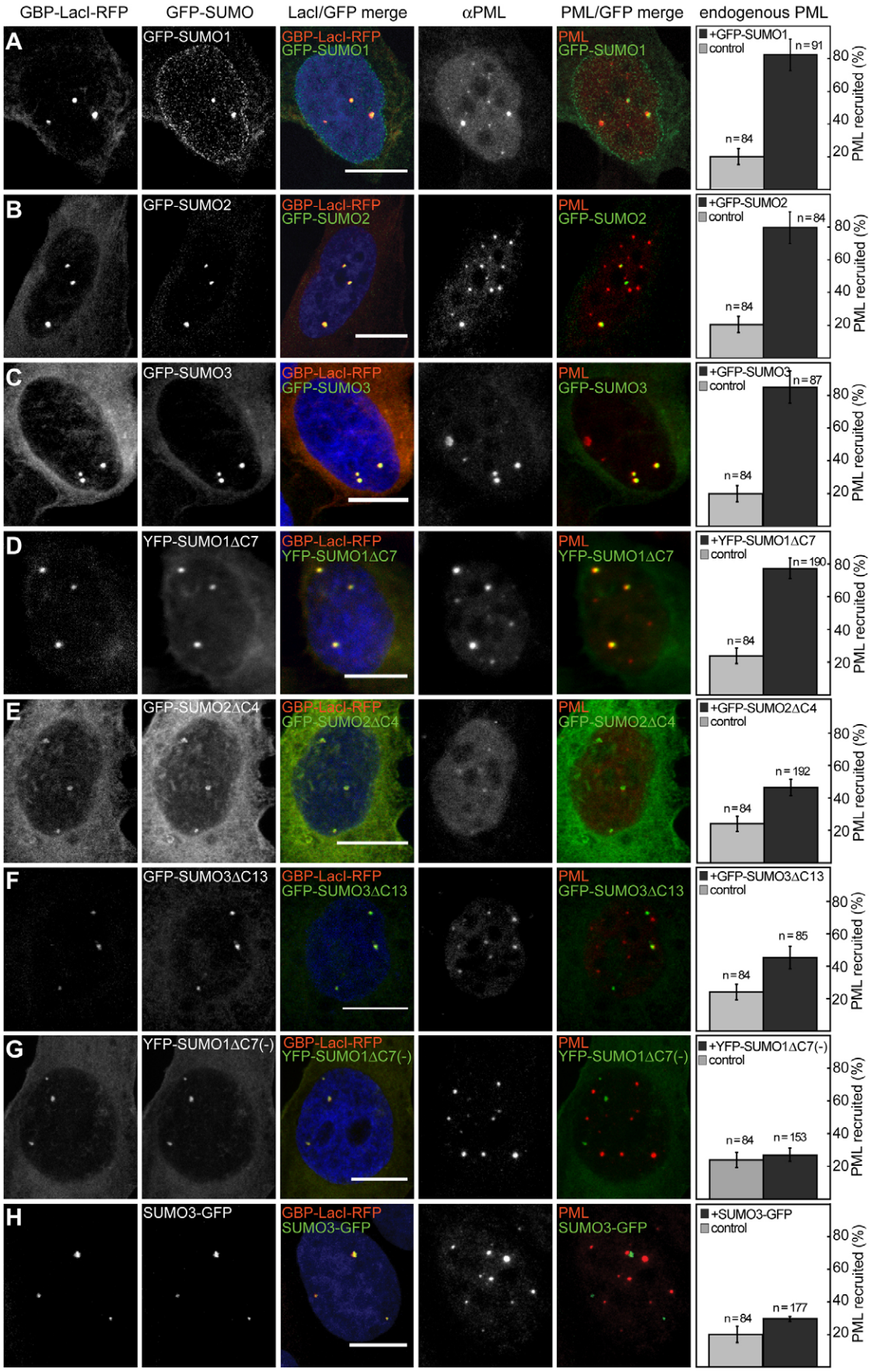

Fig. 3. See next page for legend.

SUMO1 interactions are essential for APB assembly

Because impairment of sumoylation disrupts PML-NB formation, and sumoylated telomeric proteins are crucial for the formation of APBs in ALT-positive cells (Potts and Yu, 2007; Shen et al., 2006), we investigated the effect of tethering the SUMO domain to the *lac*O-tagged telomeres. Recruitment of GFP-tagged SUMO1, SUMO2 or SUMO3 constructs was clearly sufficient to initiate the formation of APBs, as judged by the degree of colocalization of the three GFP–SUMO variants with endogenous PML, endogenous Sp100 and endogenous Rad17, i.e. 80–85% (Fig. 3A–C), 60–80% (supplementary material Fig. S2A–C) and 40–50% (supplementary material Fig. S2D–F), respectively. Structural APB components, such as PML and Sp100, are subject to sumoylation and, at the same time, contain SUMO-interacting motifs (SIMs) (Hecker et al., 2006; Knipscheer et al., 2008; Shen et al., 2006). Thus, in these experiments the effect of GFP–SUMO that was covalently conjugated to its target proteins and non-covalent interactions through the SIMs could not be distinguished (supplementary material Fig. S3). Accordingly, we investigated SUMO constructs that could not be conjugated to other proteins. The covalent attachment of SUMO occurs after cleavage of its C-terminus, exposing a Gly-Gly motif that becomes bound to a lysine residue of the target protein (Geiss-Friedlander and Melchior, 2007; Muller et al., 2001). The YFP–SUMO1ΔC7, GFP–SUMO2ΔC4 and the GFP–SUMO3ΔC13 mutants lack the C-terminal double-glycine motif and can no longer be attached to target proteins (Ayaydin and Dasso, 2004; Lin et al., 2006; Mukhopadhyay et al., 2006). Tethering the SUMO1ΔC7 mutant to the *lac*O-labeled telomeres resulted in APB formation with an efficiency that was similar to that of the conjugable wild-type SUMO1 construct ($77\pm6\%$ compared with $82\pm10\%$ colocalization with endogenous PML, Fig. 3A,D). Thus, the interaction of an isolated SUMO1 domain with the SIMs of other proteins was sufficient for the APB nucleation event. By contrast, the non-conjugable mutants of SUMO2 and SUMO3 were significantly less efficient in this respect, yielding colocalization with endogenous PML of $46\pm5\%$ (GFP–SUMO2ΔC4) and $45\pm7\%$ (GFP–SUMO3ΔC13) (Fig. 3E,F). To test whether SIM–SUMO1 interactions are indeed essential for the de novo APB assembly, the YFP–SUMO1ΔC7(-) variant was evaluated. This variant was constructed by replacing the residues Val38 and Lys39 with alanine residues. These residues are part of the second β-strand of SUMO1, which is crucial for SIM binding, as shown in several studies (e.g. Perry et al., 2008; Song et al., 2005). Accordingly, YFP–SUMO1ΔC7(-) can neither be conjugated to another protein nor bind to a SIM. As shown in Fig. 3G, tethering this construct to the telomeres did not increase colocalization with endogenous PML over background levels. Thus, a SIM interaction with SUMO1 is a central component of APB nucleation. This conclusion is in line with the behavior of yet another type of SUMO construct, namely a C-terminally tagged GFP fusion of SUMO3 (Fig. 3H). This fusion protein appeared to be mostly resistant to cleavage of the C-terminus during the maturation process because it was not conjugated (supplementary material Fig. S3). Interestingly, this variant was also unable to induce de novo APB assembly upon telomere recruitment, which might be due to interference of the C-terminal GFP tag with SIM binding.

Fig. 3. Initiation of APB formation by recruitment of the SUMO domain. After co-transfection of GBP–LacI–RFP and GFP– or YFP–SUMO constructs, cells were subjected to immunostaining for endogenous PML protein in order to detect APB formation on CLSM images from the degree of colocalization between the PML signals and the GFP– or YFP–SUMO label at the three telomeres. The colocalization background signal was $19\pm5\%$ measured by transfections with GBP–LacI–RFP and the isolated GFP domain. (**A**) GFP–SUMO1, $82\pm10\%$ colocalization ($P<0.0001$). (**B**) GFP–SUMO2, $80\pm10\%$ colocalization ($P<0.0001$). (**C**) GFP–SUMO3, $85\pm10\%$ colocalization ($P<0.0001$). (**D**) Non-conjugable YFP–SUMO1ΔC7, $77\pm6\%$ colocalization ($P<0.0001$). (**E**) Non-conjugable GFP–SUMO2ΔC4, $46\pm5\%$ colocalization ($P<0.0001$). (**F**) Non-conjugable GFP–SUMO3ΔC13, $45\pm7\%$ colocalization ($P<0.0005$). (**G**) Non-conjugable and not SIM-interacting YFP–SUMO1ΔC7(-) with amino acid exchanges V38A/K39A that prevent the recognition by SIMs, $27\pm4\%$ colocalization ($P=0.16$). (**H**) Non-conjugable C-terminal-tagged SUMO3–GFP (see also supplementary material Fig. S3), $30\pm4\%$ colocalization ($P=0.07$). Scale bars: 10 μm. All error bars show the s.d.

De novo APB formation can be induced with high efficiency by recruiting the shelterin components TRF1 and TRF2, and recombination factor NBS1, but not Rad9, Rad51 or Rad17

Other known APB components were tested for their capability to induce the assembly of PML-NBs when recruited to telomeres. First, the telomere repeat binding factors 1 and 2 (TRF1 and TRF2, respectively), were investigated (Fig. 4A,B). Both TRF1 and TRF2 bind to telomeric repeats and are therefore present in endogenous APBs. Tethering these factors resulted in a strong increase of colocalization with endogenous PML, with TRF2 being somewhat more efficient than TRF1 ($85\pm7\%$ colocalization with GFP–TRF2 and $70\pm8\%$ with GFP–TRF1, Fig. 4A,B).

Because APBs are characterized by the presence of several DNA repair and recombination proteins, the propensity of such proteins to drive PML-NB assembly at *lac*O-tagged telomeres was examined. The recombination factors NBS1 and Rad51, as well as the DNA repair factors Rad9 and Rad17, were tethered to the *lac*O arrays as GFP fusions (Fig. 4C–F; Table 1). Recruitment of NBS1, which is a central component of the Mre11–Rad50–Nbs1 (MRN) repair and recombination complex, increased endogenous PML levels at the *lac*O telomeres with a high efficiency to $83\pm9\%$ (Fig. 4C) (Jiang et al., 2005; Jiang et al., 2007; Wu et al., 2003). Rad51 is a central player in DSB repair through homologous recombination and is also involved in normal telomere function, presumably by promoting t-loop formation (Verdun and Karlseder, 2007; West, 2003). Furthermore, Rad51 is present in APBs (Yeager et al., 1999). The recruitment of GFP-tagged Rad51 led only to a small increase of endogenous PML at these telomeres to $40\pm4\%$ (Fig. 4D). The Rad9 and Rad17 proteins are part of the RFC–Rad17–9-1-1 complex that participates in the DNA damage response, plays a role in telomere stability and is a component of APBs (Nabetani et al., 2004; Pandita et al., 2006; Parrilla-Castellar et al., 2004). Enriching GFP–Rad9 at the *lac*O-labeled telomeres resulted in subsequent recruitment of endogenous PML of $59\pm6\%$ (Fig. 4E). In contrast to the other investigated proteins, recruitment of GFP–Rad17 did not initiate the assembly of PML-NBs (Fig. 4F).

The composition of de novo APBs is indistinguishable from endogenous APBs

To assess whether the de-novo-assembled APBs also contain endogenous proteins involved in DNA repair and recombination, we investigated their composition by immunostaining (Fig. 5; Table 1). NBS1, Rad17 and Rad9, all bona fide components of functional APBs (Jiang et al., 2007; Jiang et al., 2009; Nabetani et al., 2004; Wu et al., 2003), were enriched between twofold

(NBS1, Fig. 5A) and approximately fourfold (Rad9, Fig. 5B) after GFP–PML recruitment. Thus, our de novo assembly approach resulted in PML-NBs associated at telomeres that were equivalent to APBs in terms of their protein composition by all criteria reported for endogenous APBs in the literature.

APB components can be assembled efficiently at a pericentric *lac*O integration site by targeting PML, TRF1, TRF2 or NBS1 to this locus

In order to examine whether the assembly of APB proteins requires the telomeric location of the *lac*O array, the U2OS cell clone F42B8 was investigated; this clone has one *lac*O array insertion at the pericentric region of chromosomes 2p (supplementary material Fig. S4) (Jegou et al., 2009). These cells showed a higher level of colocalization of endogenous PML with the *lac*O arrays (44±6%) compared with the telomeric *lac*O sequences (supplementary material Fig. S5A). This is in line with findings that described the colocalization of PML-NBs with pericentric heterochromatin (Everett et al., 1999; Luciani et al., 2006) and the previously reported interaction of heterochromatin protein 1 (HP1) with PML-NBs, which is also enriched at these sites (Hayakawa et al., 2003). Whether LacI-bound *lac*O loci per se have an increased propensity for association with PML-NBs is not clear. According to a previous study, LacI–GFP-tagged *lac*O arrays display no preferred colocalization with PML-NBs in clones of the human HT-1080 sarcoma cell line for integration sites at 13q22, 5p14, 3q26.2, 13p and 1q11 (Chubb et al., 2002). By contrast, investigations of a baby hamster kidney cell line with a *lac*O array at unknown genomic localization showed an association of PML-NBs with this region (Tsukamoto et al., 2000). Recruiting GFP–PML to the pericentric *lac*O array enriched endogenous SUMO isoforms to an extend that was similar to that measured for the telomeric *lac*O loci. (supplementary material Fig. S5B,C). Furthermore, TRF1 and TRF2 were similarly efficient in the subsequent recruitment of endogenous PML to the pericentric locus as they were at telomeric sites (Fig. 4A,B; supplementary material Fig. S6A,B). A comparable result was obtained when tethering NBS1 to the pericentric *lac*O array (supplementary material Fig. S6C), whereas GFP-tagged Rad51 could not initiate PML-NB formation at this locus (supplementary material Fig. S6D). We then tested whether the accumulation of endogenous APB marker proteins at pericentric regions upon GFP–PML recruitment was different. Remarkably, the protein composition of the nuclear bodies induced by recruitment of GFP–PML to the pericentric *lac*O arrays revealed that all factors were enriched under these conditions to a similar or even higher degree than at the telomeric sites (Fig. 5, right-hand panels). Thus, the de-novo-assembled nuclear bodies at the pericentric chromatin locus had an APB-like protein composition.

APB assembly can be induced by the MMS21 SUMO E3 ligase and occurs in two steps

The SUMO E3 ligase MMS21 induces the sumoylation of several telomere-repeat-associated proteins, such as TRF1, TRF2 and Rap1, in ALT-positive cells and thereby supports APB formation (Potts and Yu, 2007). In order to investigate the role of MMS21, we first tested for the presence of endogenous MMS21 at the *lac*O-labeled telomeres after GFP–PML recruitment (Fig. 6A). MMS21 was highly enriched upon tethering PML at these sites, resulting in an increase of colocalization from 19±3% to 68±7%. Interestingly, the nuclear bodies formed de novo at the pericentric *lac*O array contained endogenous MMS21 at similar levels to those detected at the telomeric loci (79±9% as opposed to 28±5% in the GFP control, Fig. 6B).

Next, we sought to test whether the presence of MMS21 at telomeres is sufficient to initiate APB formation in terms of recruiting endogenous PML. To this end, GFP–MMS21 was bound to the telomeric *lac*O sequences. We observed that GFP–MMS21 was highly efficient in promoting APB assembly as it increased the colocalization between telomeric *lac*O sites and endogenous PML from 19±5% to 86±9% (Fig. 6C). Notably, tethering the GFP–MMS21 to the pericentric *lac*O sites also increased the percentage of colocalizing endogenous PML from 44±6% to 95±10%, which suggests that other sumoylation targets or interaction partners might exist in addition to telomere-associated proteins (supplementary material Fig. S6E). Next, we addressed the question of whether the GFP–MMS21-induced targeting of endogenous PML protein to the telomeric *lac*O sites was accompanied by the enrichment of the DNA repair factor Rad9. The enrichment of endogenous PML and Rad9 at these sites was evaluated by immunofluorescence (Fig. 6D). Remarkably, 35±4% of the GFP–MMS21-bound telomeres colocalizing with PML did not contain Rad9 (Fig. 6D1,D3,E). By contrast, no colocalization of endogenous Rad9 with GFP–MMS21 was detected without the simultaneous presence of PML. To compare this result with the situation for native APBs, we investigated the PML:Rad9 ratio at telomere repeats identified with GFP–TRF2. The vast majority (98%) of endogenous APBs (defined as colocalization of PML and TRF2) contained Rad9, and only 0.9% of the telomeres marked by TRF2 had Rad9 but no PML (Fig. 6E). On average, we detected 54±11 telomeres per cell, of which 8±3 were associated with APBs. Endogenous APBs were found in almost every cell of the asynchronous cell population, in contrast to previous reports (Yeager et al., 1999). We note that our CLSM-based detection also included relatively small colocalization spots, as discussed in further detail elsewhere (Osterwald et al., 2011). In summary, the fully assembled functional endogenous APBs contained both PML and Rad9, which is in line with previous work showing PML colocalizing with almost all Rad9 foci in U2OS cells (Nabetani et al., 2004). In the de novo assembly process initiated by recruitment of GFP–MMS21, however, a two-step process was revealed: tethering MMS21 to the telomere led to the concomitant assembly of the PML, Sp100 and SUMO network, presumably through sumoylation of target proteins. Subsequently the DNA recombination and repair factor Rad9 was recruited, as apparent from the 35±4% of telomeres with colocalization of GFP–MMS21 and endogenous PML that did not contain endogenous Rad9 (Fig. 6D,E).

Recruitment of PML induces DNA repair synthesis at telomeric, but not at pericentric, sites

Because the ALT mechanism involves DSB repair and recombination processes, we investigated whether APB assembly induced these activities. First, we probed de-novo-formed APBs for the presence of the phosphorylated form of the histone variant H2A.X (γH2A.X), a molecular marker for DSB repair and a component of APBs (Cesare et al., 2009; Ismail and Hendzel, 2008; Nabetani et al., 2004). Indeed, an 11±7% higher γH2A.X colocalization was found, which is indicative of an increased activity in DSB repair processes (Fig. 7A). By contrast,

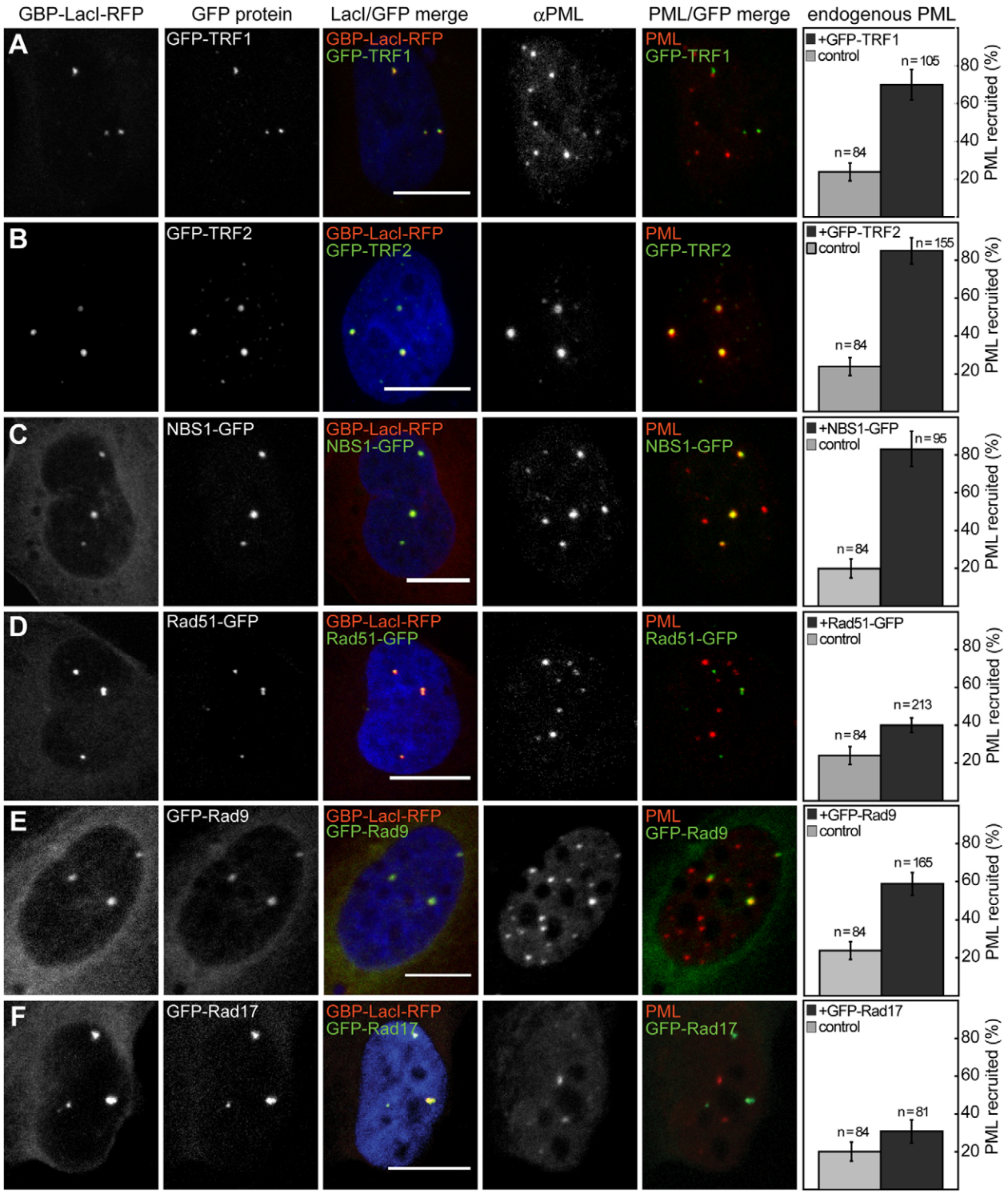

Fig. 4. Initiation of APB formation by shelterin and DNA repair and recombination proteins. Confocal images of cells that were co-transfected with GBP–LacI–RFP (column 1), the indicated GFP fusion protein (column 2, the merge of the RFP and GFP signal is shown in column 3) and immunostained for endogenous PML protein to determine APB formation (column 4). The colocalization of the GFP signal at telomeric *lac*O arrays with the immunofluorescence of endogenous PML at these sites (column 5) yielded 19±5% in the control, in which an isolated GFP domain was recruited. The propensity of proteins to induce APB formation when recruited to the telomeres as GFP fusions was evaluated in terms of colocalization with endogenous PML. This yielded values of (**A**) GFP–TRF1, 70±8% ($P<0.0001$); (**B**) GFP–TRF2, 85±7% ($P<0.0001$); (**C**) NBS1–GFP, 83±9% ($P<0.0001$); (**D**) Rad51–GFP, 40±4% ($P<0.0005$); (**E**) GFP–Rad9, 59±6% ($P<0.0001$); and (**F**) GFP–Rad17, 31±6% ($P=0.10$). Scale bars: 10 μm. All error bars show the s.d.

Table 1. APB de novo assembly and recruitment of endogenous proteins

	telomeric *lac*O arrays at 11p, 6q and 12q (F6B2 cell line)		pericentric *lac*O array at 2p (F42B8 cell line)	
Protein	Initiation of APB formation by GFP fusion protein*	Recruitment of endogenous protein to de novo APBs†	Initiation of APB-like structure assembly by GFP fusion protein*	Recruitment of endogenous protein to APB-like compartment†
PML	+++	+++	+++	n.d.
Sp100	+++	+++	n.d.	n.d.
SUMO1 wt	+++	+++	n.d.	+++
SUMO2 wt	+++	+++‡	n.d.	+++
SUMO3 wt	+++	+++‡	n.d.	+++
SUMO1ΔC7	++	n.d.	n.d.	n.d.
SUMO2ΔC4	+	n.d.	n.d.	n.d.
SUMO3ΔC13	+	n.d.	n.d.	n.d.
SUMO3–GFP	−	n.d.	n.d.	n.d.
SUMO1ΔC7(-)	−	n.d.	n.d.	n.d.
TRF1	++	n.d.	++	n.d.
TRF2	+++	n.d.	++	n.d.
MMS21	+++	++	+++	++
NBS1	+++	+	+++	++
Rad51	+	n.d.	−	n.d.
Rad9	++	++	n.d.	+++
Rad17	−	+	n.d.	++
γH2A.X	n.d.	+	n.d.	−
GFP	−	n.d.	−	n.d.

The measured degree of colocalization at the *lac*O loci was: +++, >80%; ++, >50%; +, >20%; − , no significant enrichment over background ($P>0.05$); n.d., not determined; wt, wild type.

*The indicated GFP fusion proteins were bound to the *lac*O arrays through GBP–LacI–RFP. APB formation was evaluated by immunostaining for endogenous PML at these sites, except for PML where endogenous Sp100 was measured.

†The de novo APB formation was induced by tethering GFP–PML (except for PML when GFP–Sp100 was used). Recruitment of endogenous proteins colocalizing with the GBP–LacI–RFP signal was detected by immunofluorescence.

‡The same antibody was used for detecting both the endogenous isoforms SUMO2 and SUMO3 simultaneously.

no significant enrichment of the γH2A.X signal was detected when GFP–PML was tethered to the pericentric *lac*O arrays (Fig. 7A, right-hand panel).

Second, we tested for non-replicative DNA synthesis with a 5-bromo-2′-deoxyuridine (BrdU) pulse labeling after transfection of the cells with GBP–LacI–RFP and GFP–PML, and subsequent staining with an anti-BrdU antibody. To differentiate the >50 replication foci that occur during S phase in U2OS cells from the sites of non-replicative DNA synthesis, we evaluated only those cells that displayed three or less BrdU foci (Nabetani et al., 2004). In agreement with previous reports that addressed DNA synthesis in APBs (Wu et al., 2000), the analysis of the BrdU incorporation pattern revealed a clear increase of non-replicative DNA synthesis at the telomeres at the sites of de novo formation of APBs (by $11\pm5\%$ as compared with that in the control cells, where only endogenously formed APBs were present) (Fig. 7B). Again, this increase was not observed after recruitment of PML to the pericentric *lac*O integration, where the fraction of colocalizing BrdU signal did not significantly differ from the background level (Fig. 7B, right-hand panel). Taken together, these results indicate that the de-novo-assembled nuclear bodies consist of an APB-like protein composition independent of the chromosomal site of assembly. However, these nuclear bodies have to be assembled at telomeres to induce DNA repair processes, as detected here by H2A.X phosphorylation and BrdU incorporation.

De novo APBs induce telomere repeat extension

In order to directly evaluate changes in telomere repeat length associated with de novo APB formation, fluorescence in situ hybridization (FISH) with a Cy3 fluorescently tagged peptide nucleic acid (PNA) probe against the telomere repeat sequence was conducted (Fig. 8) (Jegou et al., 2009). Owing to the heterogeneity of telomere repeat length in ALT-positive cells, a substantial number of the chromosomal ends were too short to display a detectable telomere repeat PNA-Cy3 signal. The fraction of these telomeres was determined at several time points after transfecting F6B2 cells with GBP–LacI, and either GFP–PML or a GFP-only control. The recruitment of GFP–PML to the telomeric *lac*O arrays led to an increase of the detectable $TTA(G)_3$ signal at these sites that increased over time from $57\pm7\%$ (12 hours) to $81\pm9\%$ (96 hours after transfection). In these experiments, a telomere signal was counted if it comprised >0.025% of the total PNA-Cy3 intensity in a given nucleus (Fig. 8B, left-hand panel). The telomere repeats were also examined at the pericentric *lac*O arrays. Notably, there was no significant change of the telomeric repeat signal when GFP–PML was recruited to this site (Fig. 8B, right-hand panel). This suggests that the observed increase of the $TTA(G)_3$ signal at the *lac*O-labeled telomeres can be, indeed, attributed to an extension of the telomere repeats as opposed to a PML-mediated associaton with another telomere repeat sequence. Next, a quantitative analysis of the $TTA(G)_3$ signal intensity distribution was conducted. This revealed the appearance of a fraction of telomeres (~20%) with an increased normalized repeat length of $3.4\pm0.8\%$ when GFP–PML was targeted to the telomeres (Fig. 8C). Finally, the images were inspected to determine whether the increase of telomere repeat signal at the de-novo-formed APBs was due to an induction of clustering of two or more telomeres. Within the resolution of the CLSM images, only two out of 604 (i.e. 0.3%) of the complexes showed a telomere intensity signal distribution indicative of the association of two telomeres.

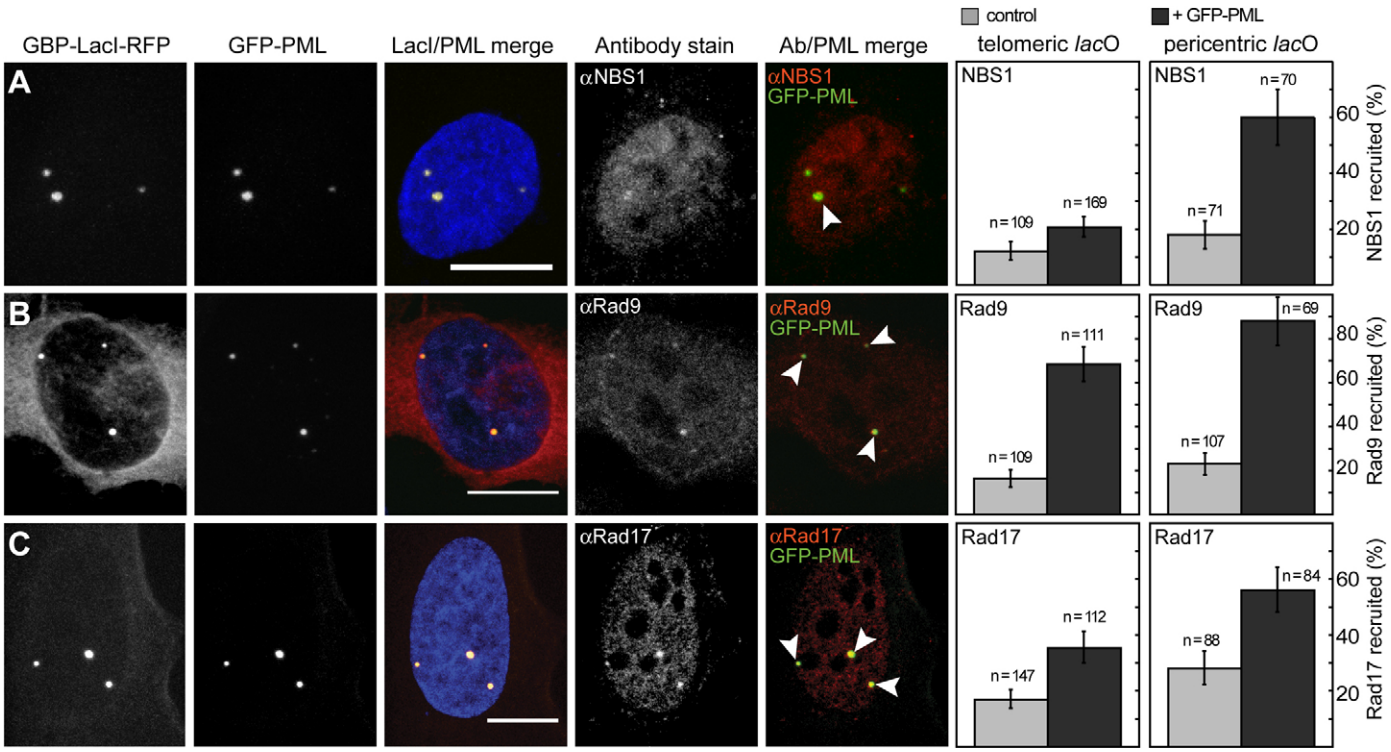

Fig. 5. Detection of endogenous proteins that are bona fide components of functional APBs. Confocal images of F6B2 cells transfected with GBP–LacI–RFP (column 1) and GFP–PML (column 2, the merge of the RFP and GFP signal is shown in column 3), to induce APB formation, and then immunostained to detect interacting endogenous DNA repair and recombination factors (column 4) from colocalization of the GFP–PML and the immunofluorescence signal (column 5). Controls were transfected with GBP–LacI–RFP only or with GBP–LacI–RFP and GFP. In order to compare the composition of non-telomeric de novo PML-NBs, the same experiments were conducted with the U2OS cell clone F42B8, which has a pericentric *lac*O integration. (**A**) Colocalization with endogenous NBS1 increased from 12±3 to 21±4% at telomeres ($P<0.05$) and from 18±5 to 60±9% at pericentromeres ($P<0.0001$). (**B**) Colocalization with endogenous Rad9 increased from 17±4 to 69±8% at telomeres and from 23±5 to 88±11% at pericentromeres ($P<0.0001$ for both analyses). (**C**) Colocalization with endogenous Rad17 increased from 17±3 to 36±6% at telomeres and from 28±6 to 56±8% at pericentromeres ($P<0.0005$ for both analyses). Scale bars: 10 μm. All error bars show the s.d.

Discussion

Here, we have investigated the assembly mechanism of APBs and their function in the ALT pathway by recruiting protein components of APBs to *lac*O-tagged telomeres in U2OS cells (Fig. 1). As described previously, the structure of the PML-NB component of APBs is determined by PML and Sp100 proteins, in conjunction with their sumoylation, to mediate the non-covalent binding of the two proteins through their SIMs (Fig. 2) (Bernardi and Pandolfi, 2007; Lang et al., 2010; Shen et al., 2006).

The shelterin components TRF1 and TRF2 were highly capable of inducing the formation of de novo APBs after enrichment at the telomeric *lac*O arrays (Fig. 4A,B). This is consistent with their requirement for APB formation in previous reports (Jiang et al., 2007). The results obtained here suggest that the amount of TRF1 and/or TRF2 accessible for protein–protein interactions or post-translational modifications, particularly sumoylation, can be a limiting factor for APB assembly at endogenous telomeres. We note that the recruitment of TRF1 and TRF2 to the *lac*O arrays also allowed us to target very short telomeres, which presumably lack parts of the shelterin complex. Enrichment of TRF1 and/or TRF2 at these telomeres could provide the required additional interaction surface for APB formation. Surprisingly, TRF2 was somewhat more efficient than TRF1 in recruiting endogenous PML, although a direct interaction between TRF1 and PML IV in the context of APB formation has been reported recently (Yu et al., 2009). However, the antibody used in the present study recognizes all PML isoforms so that a specific recruitment of PML IV might not be detected in our assay.

With our experimental system we were able to dissect the role of the three different paralogues, SUMO1, SUMO2 and SUMO3 (Fig. 3). Intriguingly, a non-conjugable SUMO1 mutant was found to be highly efficient in triggering the assembly of APB proteins, whereas mutated SUMO2 and SUMO3, which could not be conjugated to a target protein, showed only a moderate propensity to initiate this process. We speculate that the modification of telomeric proteins with SUMO1 (as mimicked in our experiments by the tethering of a non-conjugable SUMO1 mutant or the MMS21 SUMO E3 ligase) would be sufficient to initiate the formation of an APB through recruitment of SIM-containing APB components. This conclusion is further corroborated by our findings that SIM interactions of non-conjugable SUMO1 are crucial for efficient APB nucleation, in line with previous reports (Bernardi and Pandolfi, 2007; Shen et al., 2006). Moreover, our recent high-resolution three-dimensional analysis of PML-NBs revealed that the SUMO1 modification is localized preferentially in the spherical shell of PML and Sp100 protein, whereas the SUMO2 and/or SUMO3 modification was found also in the interior of PML-NBs (Lang et al., 2010). This finding points to

functional differences between the SUMO isoforms as observed here, too. Thus, we propose that PML binds SUMO1 directly through its SIM, whereas SUMO2 and SUMO3 are more weakly or indirectly bound by the main PML-NB components.

The SUMO1 modification of target proteins, as an initiating factor for APB formation, could be mediated by the MMS21 SUMO E3 ligase. This enzyme is responsible for sumoylation of the shelterin components TRF1, TRF2 and Rap1 in ALT cells

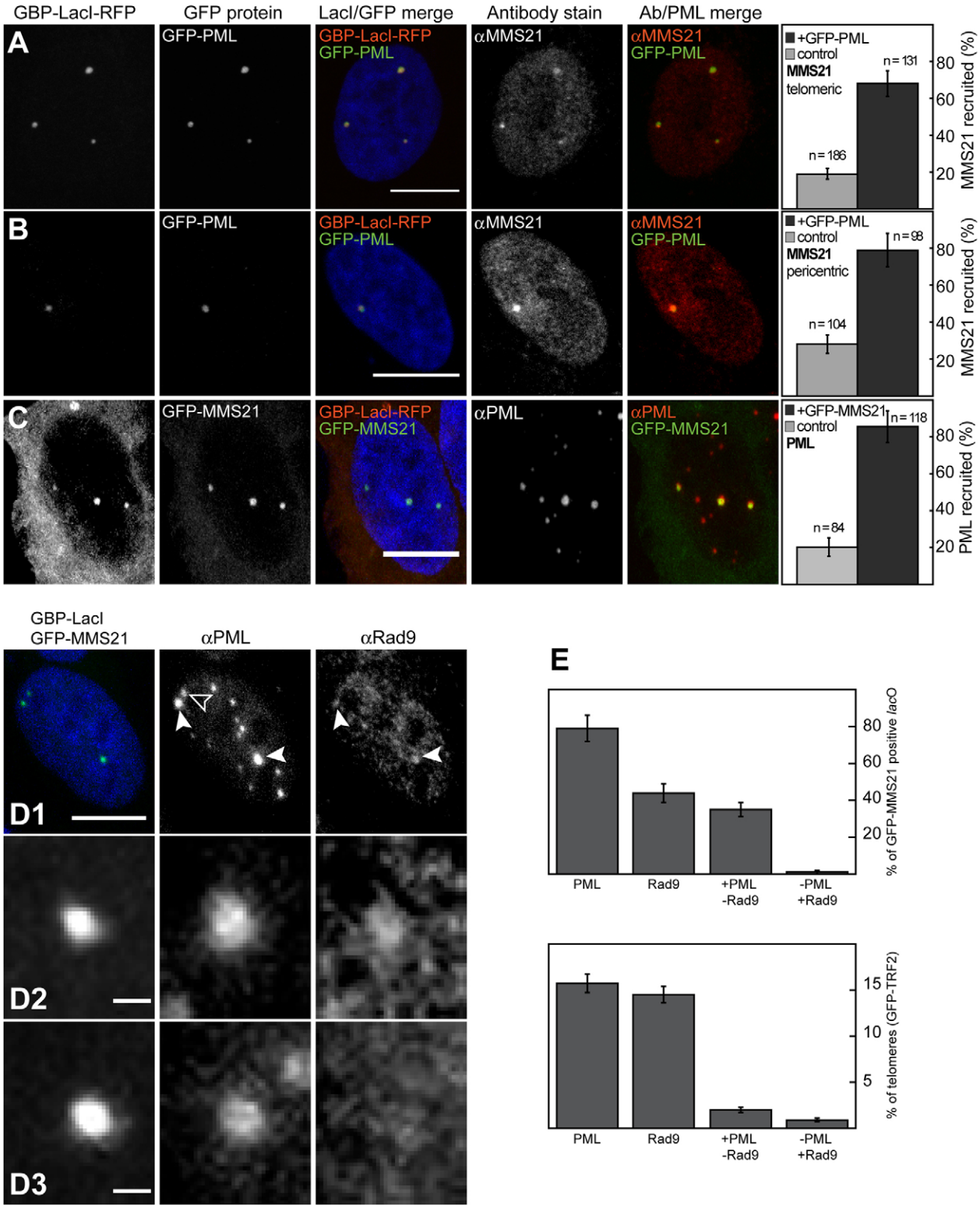

Fig. 6. See next page for legend.

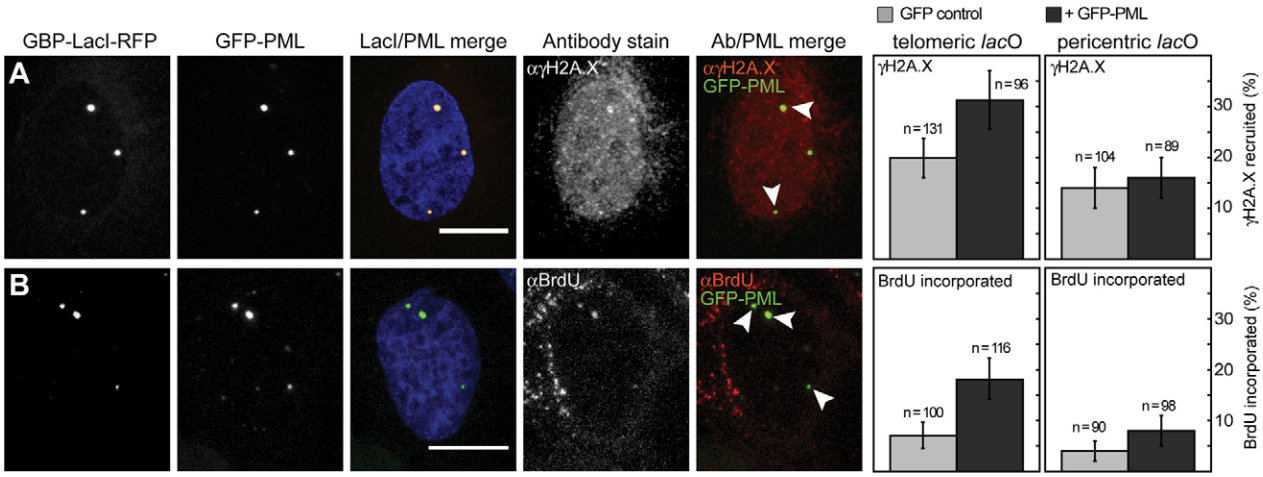

Fig. 7. Induction of DNA repair synthesis by de-novo-formed APBs. APB formation was initiated by recruiting GFP–PML to the three *lac*O-labeled telomeres in F6B2 cells and then analyzed in terms of activities associated with DSB repair and DNA synthesis at these sites. The same experiments were performed using F42B8 cells containing a pericentric *lac*O insertion. (**A**) The colocalization of APBs with the phosphorylated histone variant γH2A.X increased from 20±4% without GFP–PML transfection to 31±6%, indicative of an induction of DSB repair processes ($P<0.05$) as shown on the images for the F6B2 cell line. By contrast, there was no significant difference in F42B8 cells regarding the percentage of γH2A.X-positive *lac*O arrays with or without GFP–PML recruitment (14±4% when GFP was recruited and 16±4% after GFP–PML recruitment, $P=0.55$). (**B**) An increase in non-replicative DNA synthesis, as detected by BrdU incorporation, was found, with 18±4% APBs containing BrdU with GFP–PML transfection as compared with 7±3% in the control when only GBP–LacI–RFP was transfected ($P<0.05$). In addition to the images shown for the F6B2 cell line, the analysis revealed also cells in which not every *lac*O-labeled telomere colocalized with a BrdU signal. In addition, also cells were present that displayed BrdU-positive spots, which did not colocalize with the *lac*O arrays. Recruiting GFP–PML to a pericentric site did not induce a significant change in the portion of these sites colocalizing with the BrdU signal (4±2% with only GFP and 8±3% with GFP–PML recruited, $P=0.38$). Scale bars: 10 μm. All error bars show the s.d.

and can auto-sumoylate itself (Andrews et al., 2005; Potts and Yu, 2005; Zhao and Blobel, 2005). In support of this model, recruitment of MMS21 was found to initiate APB formation as efficiently as the SUMO1 domain (Fig. 3A,D; Fig. 6C), indicating that MMS21 promotes APB assembly through a recruitment and not a maintenance mechanism (Potts and Yu, 2007). Thus, the stabilization and spreading of the APB protein interaction network could occur through a positive-feedback loop, including binding of PML and Sp100 to sumoylated proteins mediated by their SIMs. Surprisingly, tethering MMS21 to the pericentric site was as efficient in promoting accumulation of PML protein as it was at the tagged telomeres (Fig. 6C; supplementary material Fig. S6E). Furthermore, endogenous MMS21 accumulated after enrichment of PML at both the telomeric and the pericentric sites (Fig. 6B). These findings could be related to the existence of additional targets for MMS21-mediated sumoylation, apart from the shelterin proteins, that could also play a role in APB assembly. Alternatively, the mutual recruitment of MMS21 and PML could involve the capability of MMS21 to sumoylate itself followed by the SIM-directed binding of PML. Interestingly, in addition to MMS21, the PML protein itself also possibly has a SUMO E3 ligase activity that could further amplify this propagation process (Quimby et al., 2006). In agreement with this view, PML-NBs have been described as 'hotspots' for sumoylation in the nucleus (Saitoh et al., 2006; Van Damme et al., 2010). Moreover, this model is supported by the observation that APB formation is initiated at the *lac*O arrays in our experiments, but subsequently extends further to include both the *lac*O arrays and the telomere repeats in the de-novo-formed APBs (supplementary material Fig. S1B) (Jegou et al., 2009; Lang et al., 2010).

Investigating the role of DNA recombination and repair factors showed that the recombination protein NBS1 was highly capable of inducing PML binding to telomeres when recruited as a GFP construct (Fig. 4C). However, the level of endogenous NBS1 was only slightly increased in de-novo-formed APBs by ~10% over the background (Fig. 5A). This clearly distinguishes this protein from the more abundant proteins PML and Sp100. In previous studies, interactions of NBS1 with Sp100 and TRF1 or TRF2

Fig. 6. MMS21 induced de novo APB assembly. Cells were co-transfected with GBP–LacI–RFP or GBP–LacI and GFP fusions of either PML or the SUMO E3 ligase MMS21. Subsequently, samples were stained with the indicated antibodies. (**A**) Nuclear body formation was induced by recruitment of GFP–PML to the telomeric *lac*O arrays. The presence of endogenous MMS21 was evaluated by immunofluorescence after recruitment of GFP–PML and increased from 16±5% to 68±7% ($P<0.0001$). (**B**) Same as A, but the pericentric locus was studied. Endogenous MMS21 colocalization values were 79±9% after GFP-PML recruitment compared with 28±5% in the GFP control ($P<0.0001$). (**C**) Recruitment of GFP–MMS21 with GBP–LacI–RFP to the *lac*O-labeled telomeres induced 86±9% colocalization with endogenous PML protein ($P<0.0001$). (**D**) GFP–MMS21 was tethered to the *lac*O arrays by co-transfection with the GBP–LacI construct. Colocalization of endogenous PML and Rad9 proteins with the GFP–MMS21-bound *lac*O arrays was detected by immunofluorescence. The majority of the *lac*O-tagged telomeres showed a colocalization with endogenous PML after GFP–MMS21 recruitment (indicated by arrows in D1, magnifications are shown in D2 and D3), whereas endogenous Rad9 was found only at a fraction of these sites (filled arrows in D1, a magnification is shown in D2). (**E**) Upper panel: Quantification of PML and Rad9 colocalization after GFP–MMS21 tethering ($n=182$ *lac*O-tagged telomeres). Lower panel: Analysis of endogenous APBs, identified by transfection of GFP–TRF2, in U2OS cells revealed that 16±1% of telomeres colocalized with PML and 15±1% with Rad9. A total of 2.0±0.3% telomeres were associated with only PML, and 0.9±0.2% with only Rad9 ($n=1722$ telomeres). Note the different scale of the *y*-axis. Scale bars: 10 μm (A–C,D1); 0.5 μm (D2,D3). All error bars show the s.d.

have been found to be required for recruiting the DNA repair factors Mre11, Rad50 and Brca1 to APBs (Naka et al., 2002; Wu et al., 2003; Zhu et al., 2000). This process seems to be tightly regulated in the endogenous environment as we observed a higher enrichment of endogenous NBS1 after recruiting GFP–PML to a pericentric site, which might lack specific inhibitory mechanisms. In addition to its DNA repair and recombination activity, NBS1 could target PML-NB assembly to certain telomeres at which it is enriched. This might lead to a DSB-repair-mediated elongation at these sites. Furthermore, the strong accumulation of PML protein after tethering of NBS1 to the pericentric *lac*O array supports an ALT independent relationship between DSB signaling and PML-NB formation, as suggested previously (Dellaire and Bazett-Jones, 2004; Dellaire and Bazett-Jones, 2007). Thus, the persistent deposition of NBS1 at a chromatin locus might mimick a DNA DSB situation (Soutoglou and Misteli, 2008).

The homologous recombination (HR) factor Rad51 plays an important role in HR-mediated DSB repair as it forms nucleoprotein filaments on single-stranded DNA to promote the pairing of homologous strands and strand exchange. It was one of the first recombination factors to be described as an APB component in ALT cells (Yeager et al., 1999). Interestingly, recruitment of this factor to the telomeric *lac*O arrays promoted APB formation only weakly (Fig. 4D). This is consistent with a previous report showing that siRNA-mediated knockdown of Rad51 in U2OS cells does not lead to a disruption of APBs (Potts and Yu, 2007). With respect to the assembly mechanism, this suggests a classification of APB proteins into those that are capable of initiating the assembly and others that are only recruited subsequently. This model also accounts for the results obtained upon testing the repair factors Rad9 and Rad17. For these proteins, the accumulation of endogenous proteins in the de-novo-formed APBs was higher (Fig. 5B,C) than the increase in the level of endogenous PML proteins when GFP–Rad9 and GFP–Rad17 were enriched at the telomeres (Fig. 4E,F). Thus, both Rad9 and Rad17 are less efficient as initiation factors for APBs but readily assemble at these sites once these complexes are formed. This view is supported by our finding that Rad9 binding to telomeres correlated with the presence of PML but not vice versa (Fig. 6). We conclude that during APB formation, the assembly of structural nuclear body core components PML and Sp100 precedes the subsequent binding of DNA repair and recombination factors according to the mechanism depicted in Fig. 9. The comparison of de-novo-assembled nuclear bodies after recruitment of GFP–PML to a pericentric *lac*O array revealed that the essential features of the assembly process were independent of the chromosomal site. SUMO1, SUMO2 and SUMO3, NBS1, Rad9, Rad17 and MMS21 were enriched at both the telomeric and the pericentric sites to similar levels. This points to a self-organization process for the genome-associated structural PML-NB subcompartment through stochastic interactions of the constituting components, as opposed to a

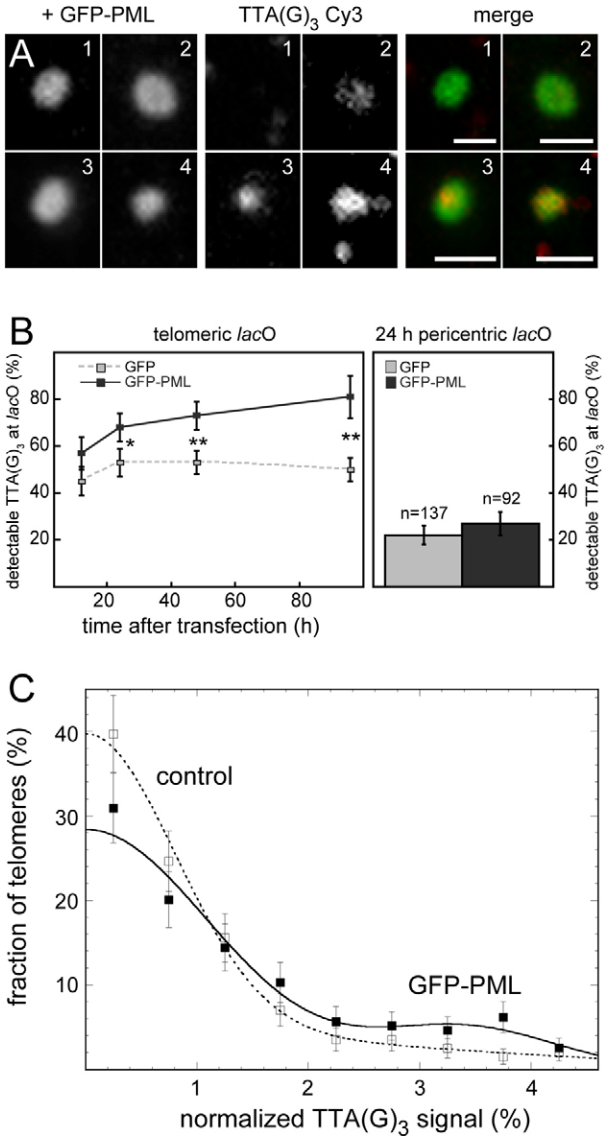

Fig. 8. Induction of telomere repeat extension by de-novo-formed APBs. Changes in the length of the telomere repeat sequence $TTA(G)_3$ upon de novo APB assembly were evaluated in FISH experiments with a Cy3-labeled PNA probe complementary to this sequence. In the control, GBP–LacI was co-transfected with the isolated GFP domain instead of GFP–PML. (**A**) Four examples (numbers 1–4) for the evaluation of the telomere repeat length at the *lac*O-tagged telomeres are depicted. The normalized telomere length was determined as the intensity ratio of the $TTA(G)_3$–Cy3 fluorescence intensity at a telomere colocalizing with the *lac*O-bound GFP(–PML) label to that of the total Cy3 signal in a given nucleus. A normalized telomere repeat signal of <0.025% (equivalent to two times the Cy3 background signal), as in telomere 1, was considered a non-detectable telomere signal. By contrast, the other three telomeres had values of 0.5% (2), 1.4% (3) and 3.7% (4). Scale bars: 0.5 μm. (**B**) The percentage of detectable telomeric repeats was determined at 12 (n=141 for GFP, n=116 for GFP–PML), 24 (n=167 for GFP, n=184 for GFP–PML), 48 (n=221 for GFP, n=202 for GFP–PML) and 96 hours (n=220 for GFP, n=102 for GFP–PML) after transfection of the telomeric-*lac*O-containing F6B2 cells and revealed an increase after GFP–PML recruitment compared with the GFP-only control. *P<0.01; **P<0.0001. This was not observed when recruiting GFP–PML to pericentric sites in F42B8 cells as determined 24 hours after transfection (control GFP, 22±4%; GFP–PML recruited, 27±5%, P=0.43). (**C**) The resulting distribution of detectable telomere signal intensities (i.e. ⩾0.025% telomere repeat signal as shown in A) was fitted to a one- or two-component Gauss distribution. Approximately 20% of telomeres with an increased normalized repeat length of 3.4±0.8% appeared when APB formation was induced through recruitment of GFP–PML. All error bars show the s.d.

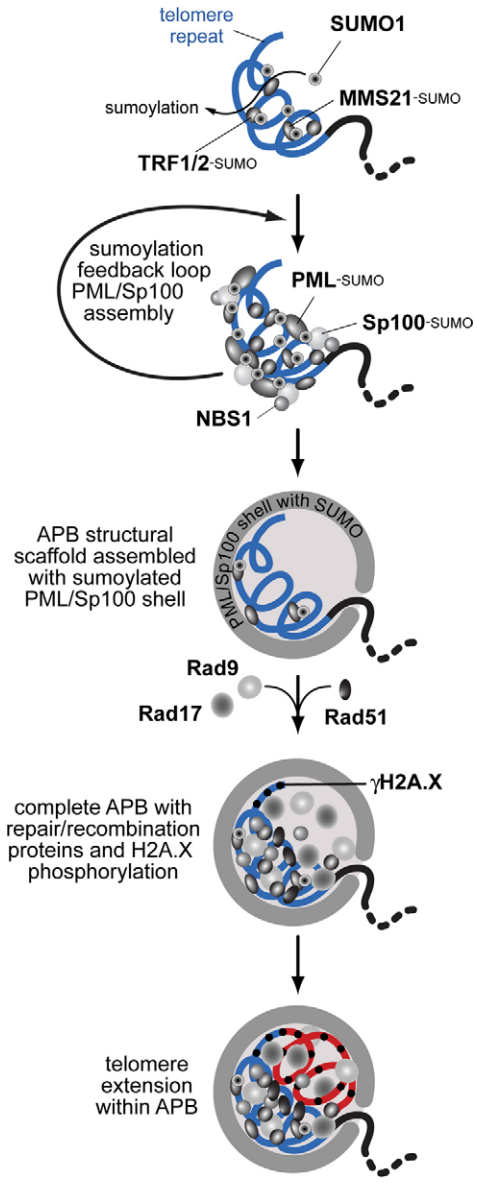

Fig. 9. Model for the mechanism of APB assembly and telomere elongation. As described in the text, APB formation can be initiated by the recruitment of the isolated SUMO1 domain or the SUMO E3 ligase MMS21, as well as the telomeric proteins TRF1 and TRF2. Accordingly, we propose that the assembly of an APB is initiated by sumoylation of telomeric proteins. The initial nucleation event triggers a feedback mechanism that leads to the enrichment of PML and Sp100. Additional auto-sumoylated MMS21 is recruited by the SIMs of PML and Sp100, so that the SUMO1-dense region is amplified and propagates to comprise the complete telomere repeat sequence. Our data also suggest that NBS1 is one of the initiating factors for APB formation. Once the structural components of the APB are fully assembled, other proteins, such as the DNA recombination and repair factors Rad51, Rad9 and Rad17, are recruited to this binding platform. This results in the formation of an APB complex that is functional in telomere extension in a DNA repair process that involves non-replicative DNA synthesis as shown here by the phosphorylation of H2A.X, the incorporation of BrdU and the increase of telomeric DNA.

defined sequential order of binding events (Fig. 9) (Dinant et al., 2009; Hancock, 2004; Hebert and Matera, 2000; Matera et al., 2009; Misteli, 2007; Wachsmuth et al., 2008). This aspect of APB formation is very similar to that reported for Cajal nuclear bodies (Kaiser et al., 2008). It is supported by experiments on the dissociation and reassembly of PML-NBs through varying the degree of molecular crowding in their environment (Hancock, 2004). In addition to previous findings on the self-organizing properties of nuclear bodies, we propose that the APB protein interaction network is stabilized by a feedback and propagation mechanism that comprises: (1) the MMS21 SUMO E3 ligase and possibly other E3 ligases; (2) the post-translational sumoylation of PML, Sp100, telomeric proteins TRF1, TRF2 and Rap1, and MMS21 itself; and (3) the SUMO-interacting domains of PML and Sp100 (Fig. 9). In contrast to the initiating proteins, other APB proteins, such as Rad9, Rad17 and Rad51, are incorporated later, in conjunction with the phosphorylation of the H2A.X histone variant. Thus, a preassembled subset of APB components is required for the subsequent binding of other factors. This feature of the sequential assembly mechanism has been reported previously for the recruitment of Sp100 and Daxx to early G1 PML-NBs and the prior binding of the MRN complex to telomeres before APB assembly (Chen et al., 2008; Jiang et al., 2007).

The APBs assembled here by recruiting essential structural components of APBs, such as PML, Sp100 and SUMO1, to the telomere-associated *lac*O arrays were indistinguishable from their endogenous counterparts with respect to protein composition and structural organization according to all criteria reported previously. This allowed us to address the question of whether this nuclear subcompartment has an essential function within the ALT pathway. To this end, we evaluated the presence of the phosphorylated γH2A.X histone variant, as a molecular marker for DSB repair, as well as non-replicative DNA synthesis through the incorporation of BrdU into the DNA (Fig. 7). We found that the de-novo-assembled APBs were positive for these two hallmarks of DNA repair. Presumably these activities are coupled to the DNA damage response pathway, as previous work has shown that BrdU incorporation in APBs is dependent on the phosphoinositide 3-kinase (PI3K)-like kinases ATR and ATM (Nabetani et al., 2004). Finally, we showed by quantitative FISH that the recruitment of GFP–PML to the telomeric *lac*O arrays led to an increase in the telomere repeat length at these sites (Fig. 8). A fraction of the de-novo-formed APBs (10–15%) was competent in inducing telomere extension during an ~24 hour time period. This number is consistent with the result that not all of the de novo APBs contained the complete set of DNA repair and recombination factors investigated here (Fig. 5; Table 1). A longer incubation of the cells further increased the percentage of functional APBs so that ~30% of the APBs had telomere extension activity after 96 hours (Fig. 8B, left panel). As discussed above, recruitment of PML to a non-telomeric site led to the formation of a nuclear body that contained all of the tested APB proteins. However, this nuclear subcompartment was non-functional with respect to H2A.X phosphorylation and the non-replicative synthesis of telomeric DNA as there was no significant difference in BrdU incorporation and the detected telomere repeat signal (Fig. 7; Fig. 8B right panel).

Previously, a study of artificially enlarged telomere–PML-NB complexes, which form upon transfection of ALT cells with a mutated form of the herpesvirus ICP0 protein, showed that these APB structures promote the association of multiple telomeres (Draskovic et al., 2009). Our structural analysis of de-novo-assembled and endogenous APBs in U2OS cells by

conventional CLSM and high-resolution 4Pi microscopy, here and elsewhere, revealed a cap-like structure of PML protein formed around a single telomere signal in U2OS cells (Fig. 1B; supplementary material Fig. S1) (Jegou et al., 2009; Lang et al., 2010). Two separate telomere signals were only distinguishable for a small fraction of APBs (0.1-0.3%). Thus, under our experimental conditions, we did not find evidence that telomere clustering could explain the observed increase of the telomere repeat signal at the de-novo-formed APBs. Furthermore, although all APB marker proteins were present at the pericentric *lac*O arrays after PML recruitment, no additional binding of telomeres or extrachromosomal telomeric repeat (ECTR) DNA was detected. Thus, an association of ECTRs with PML and TRF2 protein in APBs, proposed previously on the basis of sucrose gradient fractionation of nuclear components after DNA damage induction and sonication, was not apparent in our system (Fasching et al., 2007). The de novo assembly of PML protein at the *lac*O-tagged telomeres induced the binding of other APB components and led to H2A.X phosphorylation, BrdU incorporation and an increase in the telomere repeat DNA signal. Accordingly, we conclude that the formation of bona fide APBs promotes the extension of the telomere repeat sequence by a DNA-repair-coupled synthesis process. Our study does not provide information on the nature of the telomere repeat template used for synthesis, i.e. whether it is intra- or inter-chromosomal or an APB-associated ECTR. Furthermore, given the large number of partially contradicting results in the literature, it is well conceivable that different telomerase-independent mechanisms for telomere repeat extension exist. In addition, certain cellular conditions could lead to the formation of telomeric PML-NBs that are incapable of promoting telomere extension. For example, APB-like colocalizations of PML-NB and telomeres have been detected in telomerase-positive human cancer cell lines upon exogenous expression of the telomerase RNA component, but other characteristics of the ALT pathway were missing (Pickett et al., 2009). Likewise, a human cell line that maintains telomeres in the absence of telomerase but without the formation of APBs has been described (Cerone et al., 2005). Thus, it will be important to further dissect the exact combination of protein factors that are sufficient to trigger telomere extension in APBs and to investigate the effects of their presence or absence. We anticipate that the experimental approach introduced here, in conjunction with RNA interference (RNAi)-based three-dimensional confocal microscopy high-content screening for genes involved in APB formation (Osterwald et al., 2011), will provide a valuable approach for subsequent studies. It will allow us to precisely identify all protein components that are sufficient to form a telomeric PML-NB subcompartment structure, as well as the additional factors needed to induce telomere extension at these sites. This will serve to select protein targets for inhibiting telomere extension, and thus cell proliferation, in tumors that make use of the ALT pathway.

Materials and Methods

Protein constructs

The cDNAs encoding TRF1, SUMO1, SUMO2, SUMO3, MMS21, Rad51, Rad9 and Rad17 were obtained from the DKFZ Genomics and Proteomics Core Facility and cloned into pcDNA-DEST53 (N-terminal GFP-tag) and pcDNA-DEST47 (C-terminal GFP tag) expression vectors (Invitrogen). Constructs for GFP–PML III and GFP–TRF2 were as described previously (Jegou et al., 2009). The other constructs were kindly provided as indicated: GFP–PML IV [Peter Hemmerich, FLI Jena, Germany (Weidtkamp-Peters et al., 2008)], GFP–CenpA [Stephan Diekmann, FLI Jena, Germany (Hemmerich et al., 2008)], GFP–Sp100 and NBS1–2GFP (Thomas Hofmann, DKFZ Heidelberg, Germany), pEYFP-SUMO1ΔC7 (Frauke Melchior, ZMBH Heidelberg, Germany). The non-SIM-interacting mutant pEYFP-SUMO1ΔC7(-) was created by site-directed mutagenesis to convert Val38 and Lys39 into alanine residues. Non-conjugable GFP–SUMO2ΔC4 and GFP–SUMO3ΔC13 constructs were created from the corresponding pcDNA-DEST53-SUMO2/3 vectors by site-directed mutagenesis, replacing the first glycine codon of the C-terminal Gly-Gly motif with a stop codon. The fluorescence three-hybrid system for recruiting GFP-tagged proteins to *lac*O arrays through GBP–LacI and GBP–LacI–RFP was provided by Chromotek (Munich, Germany).

Cell culture work, immunostaining and PNA FISH

The U2OS cell clones F6B2 and F42B8 were cultured and transfected as described previously (Jegou et al., 2009). Cells were typically fixed 24 hours after transfection with 4% paraformaldehyde in PBS buffer. For the analysis by immunostaining, cells were washed and permeabilized for 5 minutes with ice-cold 0.1% (v/v) Triton X-100 solution in PBS. After three PBS washes, cells were blocked for at least 15 minutes with 10% goat serum in PBS, the solution was removed, and the cells were incubated with appropriate dilutions of specific antibodies against γH2A.X (1:100, rabbit, Millipore), NBS1 (1:200, NB100-143, Novus Biologicals), PML (1:150, PG-M3, Santa Cruz Biotechnology), Rad9 (1:100, M-389, Santa Cruz Biotechnology), Rad17 (1:200, H-300, Santa Cruz Biotechnology), Sp100 (1:200, AB1380, Chemicon), SUMO1 (1:100, FL-101, Santa Cruz Biotechnology) or SUMO2/3 (1:200, rabbit, Abcam). For immunofluorescence of MMS21, cells were fixed with 1% paraformaldehyde, and permeabilization and blocking was conducted in 0.2% (v/v) Triton X-100 and 3% BSA in PBS for 20 minutes, and the antibody was incubated in the same buffer (1:75, Abnova, NSMCE2 MaxPab, B01). For 5-bromo-2′-deoxyuridine (BrdU) staining, cells were seeded, transfected and incubated for 1 or 2 days. Then 100 μM BrdU (Sigma-Aldrich) was added to the medium for 2 to 4 hours, the cells were fixed, permeabilized with 0.2% (v/v) Triton X-100 in PBS, denatured with 1.5 M HCl for 30 minutes and then stained with an antibody against BrdU (1:50, B44, BD Biosciences). After incubation with primary antibodies the coverslips were washed with PBS containing 0.002% (v/v) NP40. The appropriate secondary antibodies conjugated to Alexa Fluor 488 or Alexa Fluor 633 (Molecular Probes) were diluted according to the manufacturer's instructions in PBS, applied to the cells and incubated for 30–60 minutes. After another PBS wash, the coverslips were mounted with Vectashield (Vector Laboratories) or Prolong Gold antifade reagent (Molecular Probes) both containing DAPI. For telomere PNA FISH, cells were grown on a slide or coverslip, transfected, incubated for the indicated time, washed with PBS and fixed with 4% paraformaldehyde. After permeabilization with 0.2% (v/v) Triton X-100 in PBS, cells were dehydrated by a series of ethanol washes (70%, 85% and 100% ethanol), air-dried and a Cy3-labeled $(CCCTAA)_3$ PNA probe (Dako, Glostrup, Denmark) was added. Then, samples were denatured at 80℃ for 3 minutes and hybridization was conducted for at least 3 hours at 30℃. Slides were then washed consecutively with 70% formamide in 10 mM Tris-HCl pH 7.4, 2× SSC, 0.1× SSC at 55℃ and 0.05% (v/v) Tween-20 in 2× SSC. In order to enhance the GFP signal, immunofluorescence was conducted as described above using an antibody against GFP (1:500, ab290, Abcam). FISH experiments on metaphase chromosomes were conducted as described before using 200 ng of a Cy3-labeled oligonucleotide probe hybridizing to the *lac*O sequence (Jegou et al., 2009).

Confocal fluorescence microscopy, image analysis and statistical evaluation

Fluorescence images were acquired with different Leica TCS SP5 confocal laser scanning microscopes. Optical sections with spacing of 0.3 μm along the *z*-axis were recorded. Fluorescence intensities in the different color channels were analyzed on the individual *z*-slices. Cells with appropriate expression levels of the fluorescent cells were chosen. Spots were counted as colocalizing if the signal at the *lac*O array was at least twofold above the background and comprised at least two pixels with a size of 200 nm. The percentage of *lac*O arrays with colocalization was determined with the indicated value n giving the number of *lac*O arrays evaluated. Error bars were calculated as $\sqrt{n}$, which yields the standard deviation for a Poisson distribution. Data obtained from the image analysis represent averages from at least three independent experiments. In the figures, maximum intensity projections of the image stacks are shown. In order to determine whether the percentages of colocalization after recruiting the proteins of interest were significantly different from the ones obtained in the controls, the Fisher's exact test was used to calculate *P*-values.

Western blotting

A total of 5×10^6 F6B2 cells were seeded and transfected with GFP–SUMO3 or SUMO3–GFP, incubated for 24 hours, washed with PBS, incubated with ice-cold RIPA buffer for 30 minutes at 4℃ and centrifuged at 4℃. The supernatant was subjected to SDS-PAGE (12% gels) and, after blocking with 3% BSA in PBS, subjected to western blot analysis with an antibody against GFP (ab290, Abcam) according to the manufacturer's protocol.

Acknowledgements

We thank Ulrich Rothbauer, Kourosh Zolghadr, Thomas Hofmann, Jiri Bartek, Frauke Melchior, Peter Hemmerich and Stephan Diekmann for reagents and help, and Sarah Osterwald, Daniel Parisotto, Jan-Philipp Mallm, Maiwen Caudron-Herger and Thomas Höfer for discussions.

Funding

This work was supported by the project EpiSys within the BMBF SysTec program.

Supplementary material available online at
http://jcs.biologists.org/lookup/suppl/doi:10.1242/jcs.084681/-/DC1

References

Andrews, E. A., Palecek, J., Sergeant, J., Taylor, E., Lehmann, A. R. and Watts, F. Z. (2005). Nse2, a component of the Smc5-6 complex, is a SUMO ligase required for the response to DNA damage. *Mol. Cell Biol.* **25**, 185-196.

Ayaydin, F. and Dasso, M. (2004). Distinct in vivo dynamics of vertebrate SUMO paralogues. *Mol. Biol. Cell* **15**, 5208-5218.

Bernardi, R. and Pandolfi, P. P. (2007). Structure, dynamics and functions of promyelocytic leukaemia nuclear bodies. *Nat. Rev. Mol. Cell Biol.* **8**, 1006-1016.

Cerone, M. A., Autexier, C., Londono-Vallejo, J. A. and Bacchetti, S. (2005). A human cell line that maintains telomeres in the absence of telomerase and of key markers of ALT. *Oncogene* **24**, 7893-7901.

Cesare, A. J. and Reddel, R. R. (2010). Alternative lengthening of telomeres: models, mechanisms and implications. *Nat. Rev. Genet.* **11**, 319-330.

Cesare, A. J., Kaul, Z., Cohen, S. B., Napier, C. E., Pickett, H. A., Neumann, A. A. and Reddel, R. R. (2009). Spontaneous occurrence of telomeric DNA damage response in the absence of chromosome fusions. *Nat. Struct. Mol. Biol.* **16**, 1244-1251.

Chen, Y. C., Kappel, C., Beaudouin, J., Eils, R. and Spector, D. L. (2008). Live cell dynamics of promyelocytic leukemia nuclear bodies upon entry into and exit from mitosis. *Mol. Biol. Cell* **19**, 3147-3162.

Chubb, J. R., Boyle, S., Perry, P. and Bickmore, W. A. (2002). Chromatin motion is constrained by association with nuclear compartments in human cells. *Curr. Biol.* **12**, 439-445.

Collado, M., Blasco, M. A. and Serrano, M. (2007). Cellular senescence in cancer and aging. *Cell* **130**, 223-233.

de Lange, T., Lundblad, V. and Blackburn, E. (2006). Telomeres. *Cold Spring Harbor mongraph series*.

Dellaire, G. and Bazett-Jones, D. P. (2004). PML nuclear bodies: dynamic sensors of DNA damage and cellular stress. *BioEssays* **26**, 963-977.

Dellaire, G. and Bazett-Jones, D. P. (2007). Beyond repair foci: subnuclear domains and the cellular response to DNA damage. *Cell Cycle* **6**, 1864-1872.

Dinant, C., Luijsterburg, M. S., Höfer, T., Von Bornstaedt, G., Vermeulen, W., Houtsmuller, A. B. and van Driel, R. (2009). Assembly of multi-protein complexes that control genome function. *J. Cell Biol.* **185**, 21-26.

Draskovic, I., Arnoult, N., Steiner, V., Bacchetti, S., Lomonte, P. and Londono-Vallejo, A. (2009). Probing PML body function in ALT cells reveals spatiotemporal requirements for telomere recombination. *Proc. Natl. Acad. Sci. USA* **106**, 15726-15731.

Dunham, M. A., Neumann, A. A., Fasching, C. L. and Reddel, R. R. (2000). Telomere maintenance by recombination in human cells. *Nat. Genet.* **26**, 447-450.

Everett, R. D., Lomonte, P., Sternsdorf, T., van Driel, R. and Orr, A. (1999). Cell cycle regulation of PML modification and ND10 composition. *J. Cell Sci.* **112**, 4581-4588.

Fasching, C. L., Neumann, A. A., Muntoni, A., Yeager, T. R. and Reddel, R. R. (2007). DNA damage induces alternative lengthening of telomeres (ALT) associated promyelocytic leukemia bodies that preferentially associate with linear telomeric DNA. *Cancer Res.* **67**, 7072-7077.

Geiss-Friedlander, R. and Melchior, F. (2007). Concepts in sumoylation: a decade on. *Nat. Rev. Mol. Cell Biol.* **8**, 947-956.

Hancock, R. (2004). Internal organisation of the nucleus: assembly of compartments by macromolecular crowding and the nuclear matrix model. *Biol. Cell* **96**, 595-601.

Hayakawa, T., Haraguchi, T., Masumoto, H. and Hiraoka, Y. (2003). Cell cycle behavior of human HP1 subtypes: distinct molecular domains of HP1 are required for their centromeric localization during interphase and metaphase. *J. Cell Sci.* **116**, 3327-3338.

Hebert, M. D. and Matera, A. G. (2000). Self-association of coilin reveals a common theme in nuclear body localization. *Mol. Biol. Cell* **11**, 4159-4171.

Hecker, C. M., Rabiller, M., Haglund, K., Bayer, P. and Dikic, I. (2006). Specification of SUMO1- and SUMO2-interacting motifs. *J. Biol. Chem.* **281**, 16117-16127.

Hemmerich, P., Weidtkamp-Peters, S., Hoischen, C., Schmiedeberg, L., Erliandri, I. and Diekmann, S. (2008). Dynamics of inner kinetochore assembly and maintenance in living cells. *J. Cell Biol.* **180**, 1101-1114.

Henson, J. D., Neumann, A. A., Yeager, T. R. and Reddel, R. R. (2002). Alternative lengthening of telomeres in mammalian cells. *Oncogene* **21**, 598-610.

Ismail, I. H. and Hendzel, M. J. (2008). The gamma-H2A.X: is it just a surrogate marker of double-strand breaks or much more? *Environ. Mol. Mutagen.* **49**, 73-82.

Jegou, T., Chung, I., Heuvelmann, G., Wachsmuth, M., Görisch, S. M., Greulich-Bode, K., Boukamp, P., Lichter, P. and Rippe, K. (2009). Dynamics of telomeres and promyelocytic leukemia nuclear bodies in a telomerase negative human cell line. *Mol. Biol. Cell* **20**, 2070-2082.

Jiang, W. Q., Zhong, Z. H., Henson, J. D., Neumann, A. A., Chang, A. C. and Reddel, R. R. (2005). Suppression of alternative lengthening of telomeres by Sp100-mediated sequestration of the MRE11/RAD50/NBS1 complex. *Mol. Cell. Biol.* **25**, 2708-2721.

Jiang, W. Q., Zhong, Z. H., Henson, J. D. and Reddel, R. R. (2007). Identification of candidate alternative lengthening of telomeres genes by methionine restriction and RNA interference. *Oncogene* **26**, 4635-4647.

Jiang, W. Q., Zhong, Z. H., Nguyen, A., Henson, J. D., Toouli, C. D., Braithwaite, A. W. and Reddel, R. R. (2009). Induction of alternative lengthening of telomeres-associated PML bodies by p53/p21 requires HP1 proteins. *J. Cell Biol.* **185**, 797-810.

Kaiser, T. E., Intine, R. V. and Dundr, M. (2008). De novo formation of a subnuclear body. *Science* **322**, 1713-1717.

Knipscheer, P., Flotho, A., Klug, H., Olsen, J. V., van Dijk, W. J., Fish, A., Johnson, E. S., Mann, M., Sixma, T. K. and Pichler, A. (2008). Ubc9 sumoylation regulates SUMO target discrimination. *Mol. Cell* **31**, 371-382.

Lallemand-Breitenbach, V. and de The, H. (2010). PML nuclear bodies. *Cold Spring Harb. Perspect Biol.* **2**, a000661.

Lang, M., Jegou, T., Chung, I., Richter, K., Udvarhelyi, A., Münch, S., Cremer, C., Hemmerich, P., Engelhardt, J., Hell, S. W. et al. (2010). Three-dimensional structure of promyelocytic leukemia nuclear bodies. *J. Cell Sci.* **123**, 392-400.

Lin, D. Y., Huang, Y. S., Jeng, J. C., Kuo, H. Y., Chang, C. C., Chao, T. T., Ho, C. C., Chen, Y. C., Lin, T. P., Fang, H. I. et al. (2006). Role of SUMO-interacting motif in Daxx SUMO modification, subnuclear localization, and repression of sumoylated transcription factors. *Mol. Cell* **24**, 341-354.

Luciani, J. J., Depetris, D., Usson, Y., Metzler-Guillemain, C., Mignon-Ravix, C., Mitchell, M. J., Megarbane, A., Sarda, P., Sirma, H., Moncla, A. et al. (2006). PML nuclear bodies are highly organised DNA-protein structures with a function in heterochromatin remodelling at the G2 phase. *J. Cell Sci.* **119**, 2518-2531.

Matera, A. G., Izaguire-Sierra, M., Praveen, K. and Rajendra, T. K. (2009). Nuclear bodies: random aggregates of sticky proteins or crucibles of macromolecular assembly? *Dev. Cell* **17**, 639-647.

Misteli, T. (2007). Beyond the sequence: cellular organization of genome function. *Cell* **128**, 787-800.

Mukhopadhyay, D., Ayaydin, F., Kolli, N., Tan, S. H., Anan, T., Kametaka, A., Azuma, Y., Wilkinson, K. D. and Dasso, M. (2006). SUSP1 antagonizes formation of highly SUMO2/3-conjugated species. *J. Cell Biol.* **174**, 939-949.

Muller, S., Hoege, C., Pyrowolakis, G. and Jentsch, S. (2001). SUMO, ubiquitin's mysterious cousin. *Nat. Rev. Mol. Cell Biol.* **2**, 202-210.

Nabetani, A., Yokoyama, O. and Ishikawa, F. (2004). Localization of hRad9, hHus1, hRad1, and hRad17 and caffeine-sensitive DNA replication at the alternative lengthening of telomeres-associated promyelocytic leukemia body. *J. Biol. Chem.* **279**, 25849-25857.

Naka, K., Ikeda, K. and Motoyama, N. (2002). Recruitment of NBS1 into PML oncogenic domains via interaction with SP100 protein. *Biochem. Biophys. Res. Commun.* **299**, 863-871.

Osterwald, S., Wörz, S., Reymann, J., Sieckmann, F., Rohr, K., Erfle, H. and Rippe, K. (2011). A three-dimensional co-localization RNA interference screen platform to elucidate the alternative lengthening of telomeres pathway. *Biotechnol. J.*, doi: 10.1002/biot.201000474..

Pandita, R. K., Sharma, G. G., Laszlo, A., Hopkins, K. M., Davey, S., Chakhparonian, M., Gupta, A., Wellinger, R. J., Zhang, J., Powell, S. N. et al. (2006). Mammalian Rad9 plays a role in telomere stability, S- and G2-phase-specific cell survival, and homologous recombinational repair. *Mol. Cell Biol.* **26**, 1850-1864.

Parrilla-Castellar, E. R., Arlander, S. J. and Karnitz, L. (2004). Dial 9-1-1 for DNA damage: the Rad9-Hus1-Rad1 (9-1-1) clamp complex. *DNA Repair (Amst)* **3**, 1009-1014.

Perry, J. J., Tainer, J. A. and Boddy, M. N. (2008). A SIM-ultaneous role for SUMO and ubiquitin. *Trends Biochem. Sci.* **33**, 201-208.

Pickett, H. A., Cesare, A. J., Johnston, R. L., Neumann, A. A. and Reddel, R. R. (2009). Control of telomere length by a trimming mechanism that involves generation of t-circles. *EMBO J.* **28**, 799-809.

Potts, P. R. and Yu, H. (2005). Human MMS21/NSE2 is a SUMO ligase required for DNA repair. *Mol. Cell. Biol.* **25**, 7021-7032.

Potts, P. R. and Yu, H. (2007). The SMC5/6 complex maintains telomere length in ALT cancer cells through SUMOylation of telomere-binding proteins. *Nat. Struct. Mol. Biol.* **14**, 581-590.

Quimby, B. B., Yong-Gonzalez, V., Anan, T., Strunnikov, A. V. and Dasso, M. (2006). The promyelocytic leukemia protein stimulates SUMO conjugation in yeast. *Oncogene* **25**, 2999-3005.

Rothbauer, U., Zolghadr, K., Tillib, S., Nowak, D., Schermelleh, L., Gahl, A., Backmann, N., Conrath, K., Muyldermans, S., Cardoso, M. C. et al. (2006). Targeting and tracing antigens in live cells with fluorescent nanobodies. *Nat. Methods* **3**, 887-889.

Saitoh, N., Uchimura, Y., Tachibana, T., Sugahara, S., Saitoh, H. and Nakao, M. (2006). In situ SUMOylation analysis reveals a modulatory role of RanBP2 in the nuclear rim and PML bodies. *Exp. Cell Res.* **312**, 1418-1430.

Journal of Cell Science

Shen, T. H., Lin, H. K., Scaglioni, P. P., Yung, T. M. and Pandolfi, P. P. (2006). The mechanisms of PML-nuclear body formation. *Mol. Cell* **24**, 331-339.

Song, J., Zhang, Z., Hu, W. and Chen, Y. (2005). Small ubiquitin-like modifier (SUMO) recognition of a SUMO binding motif: a reversal of the bound orientation. *J. Biol. Chem.* **280**, 40122-40129.

Soutoglou, E. and Misteli, T. (2008). Activation of the cellular DNA damage response in the absence of DNA lesions. *Science* **320**, 1507-1510.

Takahashi, Y., Lallemand-Breitenbach, V., Zhu, J. and de The, H. (2004). PML nuclear bodies and apoptosis. *Oncogene* **23**, 2819-2824.

Tsukamoto, T., Hashiguchi, N., Janicki, S. M., Tumbar, T., Belmont, A. S. and Spector, D. L. (2000). Visualization of gene activity in living cells. *Nat. Cell Biol.* **2**, 871-878.

Tumbar, T., Sudlow, G. and Belmont, A. S. (1999). Large-scale chromatin unfolding and remodeling induced by VP16 acidic activation domain. *J. Cell Biol.* **145**, 1341-1354.

Van Damme, E., Laukens, K., Dang, T. H. and Van Ostade, X. (2010). A manually curated network of the PML nuclear body interactome reveals an important role for PML-NBs in SUMOylation dynamics. *Int. J. Biol. Sci.* **6**, 51-67.

Verdun, R. E. and Karlseder, J. (2007). Replication and protection of telomeres. *Nature* **447**, 924-931.

Wachsmuth, M., Caudron-Herger, M. and Rippe, K. (2008). Genome organization: Balancing stability and plasticity. *Biochim. Biophys. Acta.* **1783**, 2061-2079.

Weidtkamp-Peters, S., Lenser, T., Negorev, D., Gerstner, N., Hofmann, T. G., Schwanitz, G., Hoischen, C., Maul, G., Dittrich, P. and Hemmerich, P. (2008). Dynamics of component exchange at PML nuclear bodies. *J. Cell Sci.* **121**, 2731-2743.

West, S. C. (2003). Molecular views of recombination proteins and their control. *Nat. Rev. Mol. Cell Biol.* **4**, 435-445.

Wörz, S., Sander, P., Pfannmöller, M., Rieker, R. J., Joos, S., Mechtersheimer, G., Boukamp, P., Lichter, P. and Rohr, K. (2010). 3D Geometry-based quantification of colocalizations in multi-channel 3D microscopy images of human soft tissue tumors. *IEEE Trans. on Medical Imaging* **29**, 1474-1484.

Wu, G., Lee, W. H. and Chen, P. L. (2000). NBS1 and TRF1 colocalize at promyelocytic leukemia bodies during late S/G2 phases in immortalized telomerase-negative cells. Implication of NBS1 in alternative lengthening of telomeres. *J. Biol. Chem.* **275**, 30618-30622.

Wu, G., Jiang, X., Lee, W. H. and Chen, P. L. (2003). Assembly of functional ALT-associated promyelocytic leukemia bodies requires Nijmegen Breakage Syndrome 1. *Cancer Res.* **63**, 2589-2595.

Yeager, T. R., Neumann, A. A., Englezou, A., Huschtscha, L. I., Noble, J. R. and Reddel, R. R. (1999). Telomerase-negative immortalized human cells contain a novel type of promyelocytic leukemia (PML) body. *Cancer Res.* **59**, 4175-4179.

Yu, J., Lan, J., Wang, C., Wu, Q., Zhu, Y., Lai, X., Sun, J., Jin, C. and Huang, H. (2009). PML3 interacts with TRF1 and is essential for ALT-associated PML bodies assembly in U2OS cells. *Cancer Lett.* **291**, 177-186.

Zhao, X. and Blobel, G. (2005). A SUMO ligase is part of a nuclear multiprotein complex that affects DNA repair and chromosomal organization. *Proc. Natl. Acad. Sci. USA* **102**, 4777-4782.

Zhu, X. D., Kuster, B., Mann, M., Petrini, J. H. and de Lange, T. (2000). Cell-cycle-regulated association of RAD50/MRE11/NBS1 with TRF2 and human telomeres. *Nat. Genet.* **25**, 347-352.

Zolghadr, K., Mortusewicz, O., Rothbauer, U., Kleinhans, R., Goehler, H., Wanker, E. E., Cardoso, M. C. and Leonhardt, H. (2008). A fluorescent two-hybrid assay for direct visualization of protein interactions in living cells. *Mol. Cell Proteomics* **7**, 2279-2287.

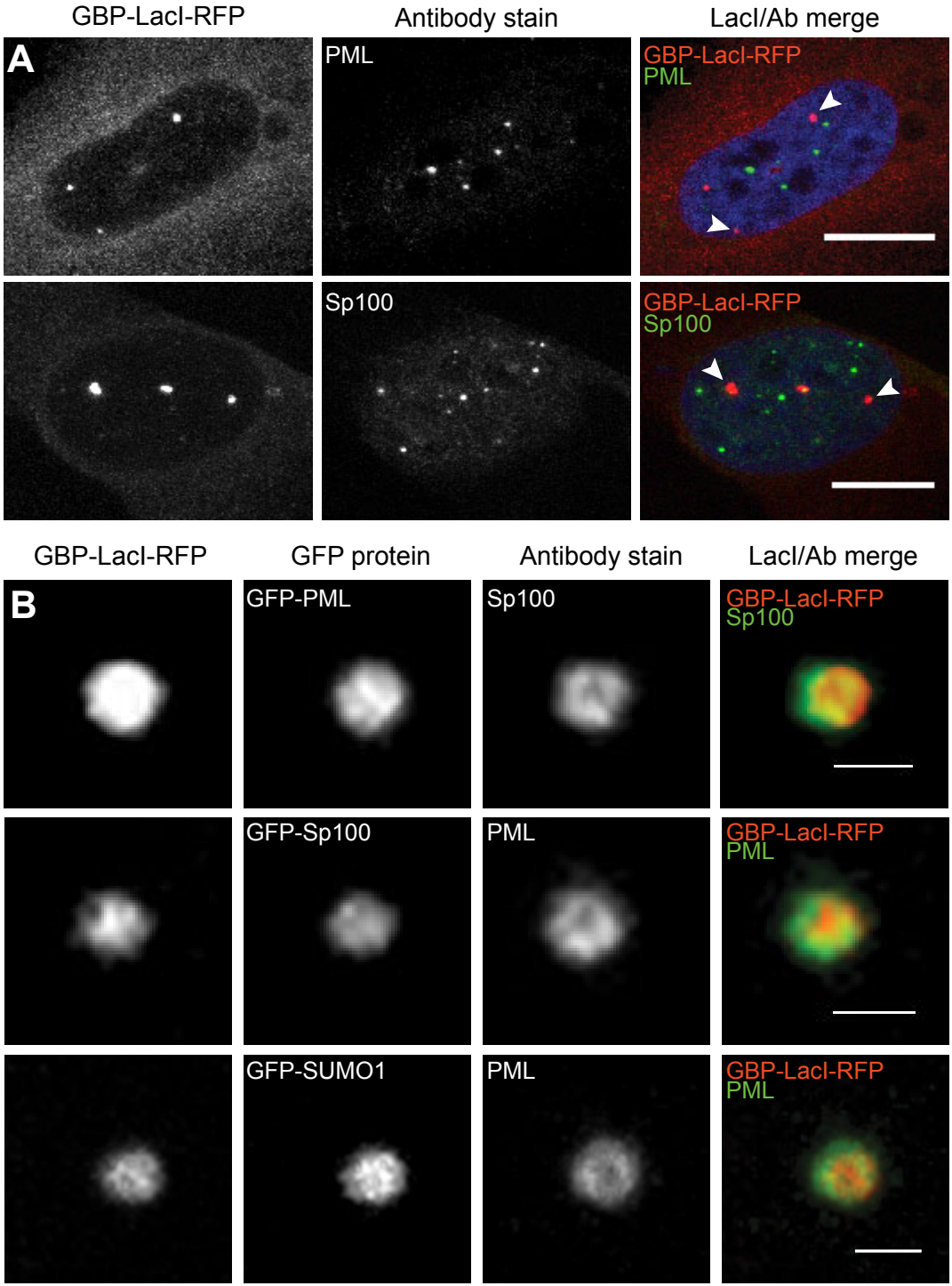
GBP-LacI-RFP
Antibody stain
LacI/Ab merge
A
PML
GBP-LacI-RFP
PML
Sp100
GBP-LacI-RFP
Sp100
GBP-LacI-RFP
GFP protein
Antibody stain
LacI/Ab merge
B
GFP-PML
Sp100
GBP-LacI-RFP
Sp100
GFP-Sp100
PML
GBP-LacI-RFP
PML
GFP-SUMO1
PML
GBP-LacI-RFP
PML

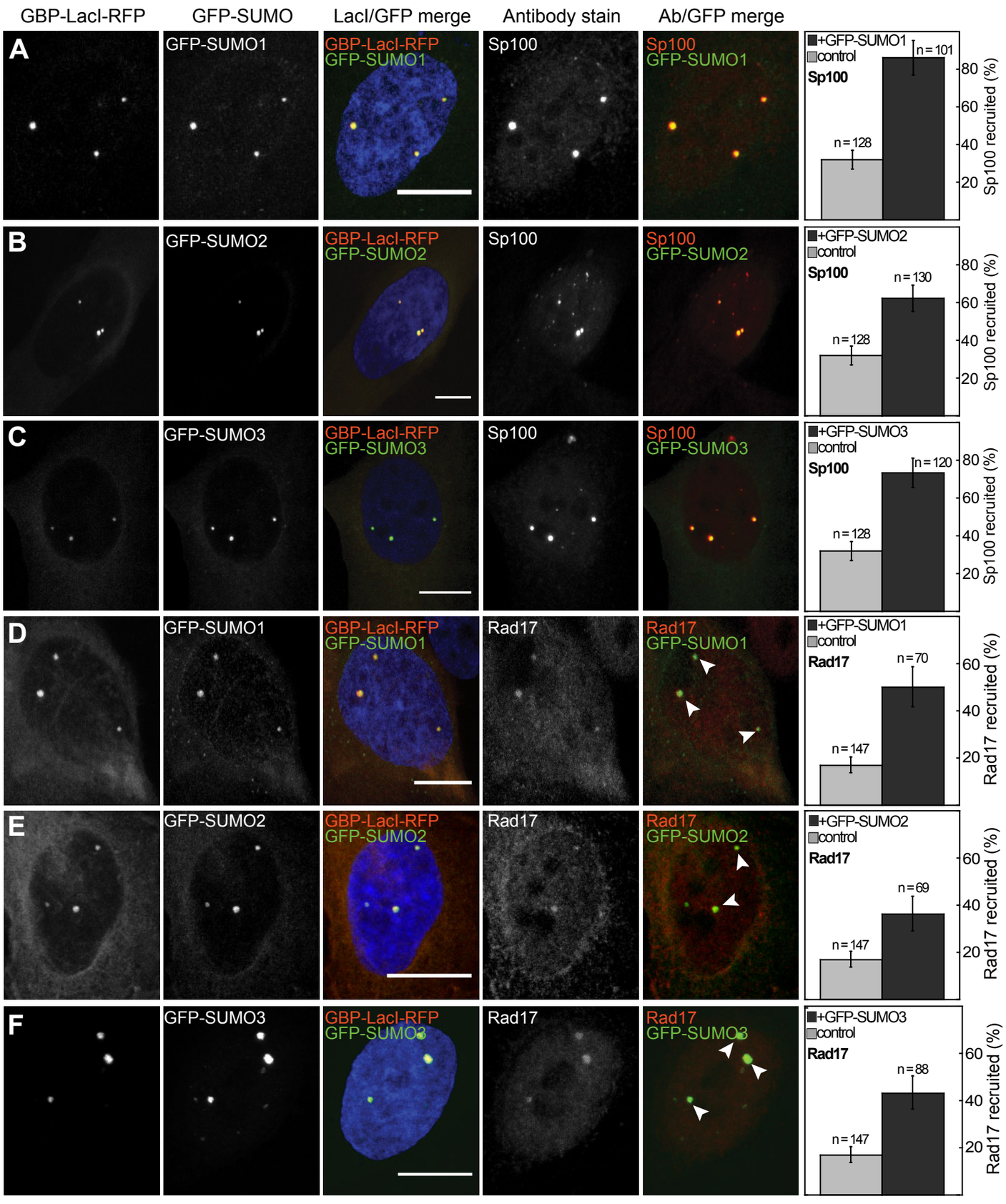
GBP-LacI-RFP
GFP-SUMO
LacI/GFP merge
Antibody stain
Ab/GFP merge
A
GFP-SUMO1
GBP-LacI-RFP
GFP-SUMO1
Sp100
Sp100
GFP-SUMO1
+GFP-SUMO1
control
Sp100
n = 101
n = 128
Sp100 recruited (%)
B
GFP-SUMO2
GBP-LacI-RFP
GFP-SUMO2
Sp100
Sp100
GFP-SUMO2
+GFP-SUMO2
control
Sp100
n = 130
n = 128
Sp100 recruited (%)
C
GFP-SUMO3
GBP-LacI-RFP
GFP-SUMO3
Sp100
Sp100
GFP-SUMO3
+GFP-SUMO3
control
Sp100
n = 120
n = 128
Sp100 recruited (%)
D
GFP-SUMO1
GBP-LacI-RFP
GFP-SUMO1
Rad17
Rad17
GFP-SUMO1
+GFP-SUMO1
control
Rad17
n = 70
n = 147
Rad17 recruited (%)
E
GFP-SUMO2
GBP-LacI-RFP
GFP-SUMO2
Rad17
Rad17
GFP-SUMO2
+GFP-SUMO2
control
Rad17
n = 69
n = 147
Rad17 recruited (%)
F
GFP-SUMO3
GBP-LacI-RFP
GFP-SUMO3
Rad17
Rad17
GFP-SUMO3
+GFP-SUMO3
control
Rad17
n = 88
n = 147
Rad17 recruited (%)

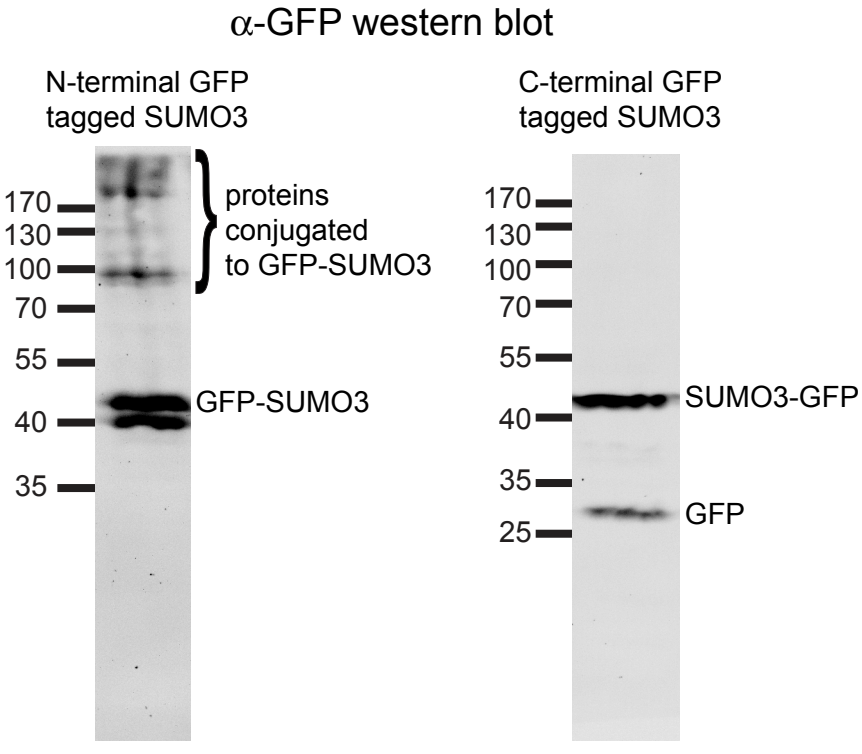
α-GFP western blot
N-terminal GFP
tagged SUMO3
C-terminal GFP
tagged SUMO3
170
130
100
70
55
40
35
proteins
conjugated
to GFP-SUMO3
GFP-SUMO3
170
130
100
70
55
40
35
25
SUMO3-GFP
GFP

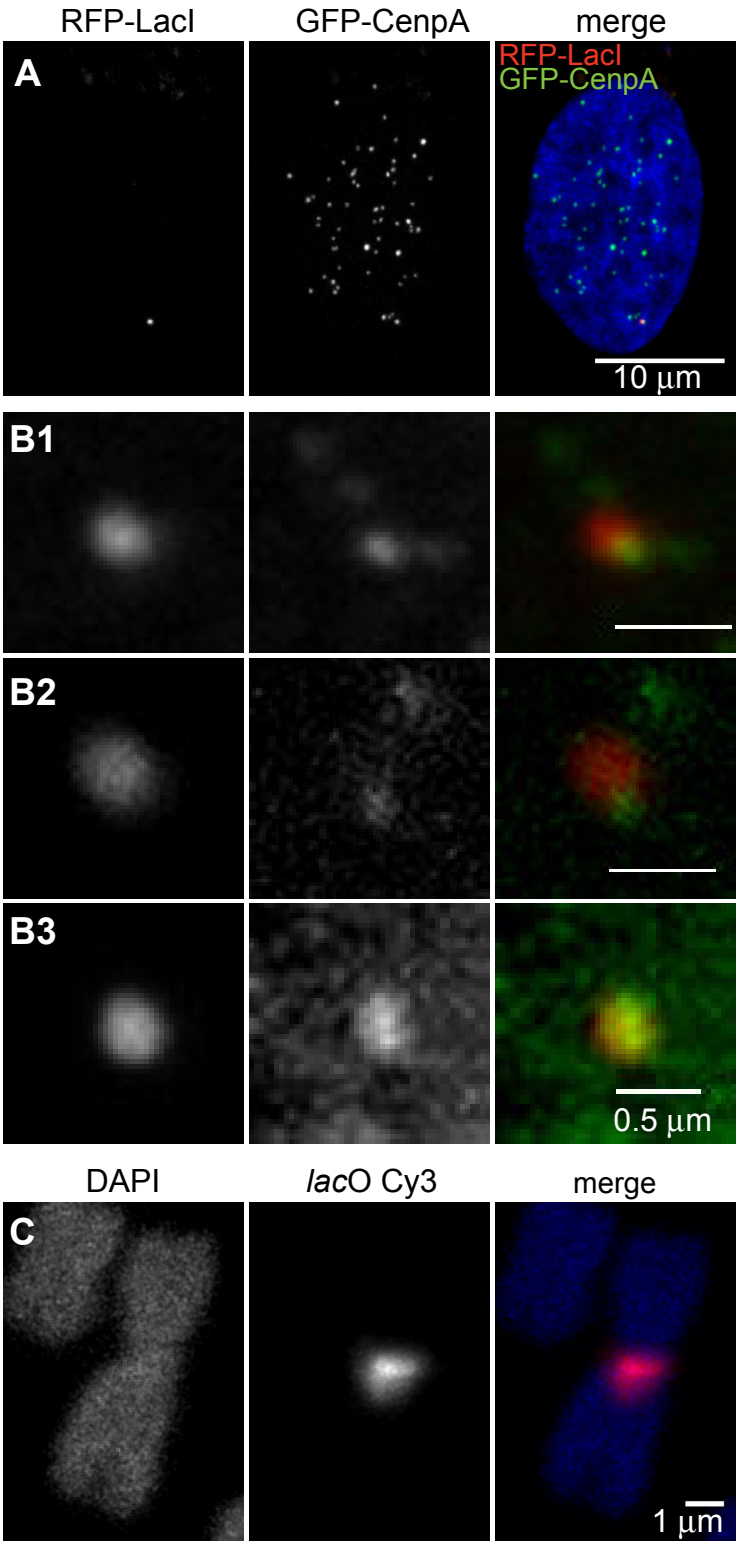
RFP-LacI
GFP-CenpA
merge
A
RFP-LacI
GFP-CenpA
10 µm
B1
B2
B3
0.5 µm
DAPI
lacO Cy3
merge
C
1 µm

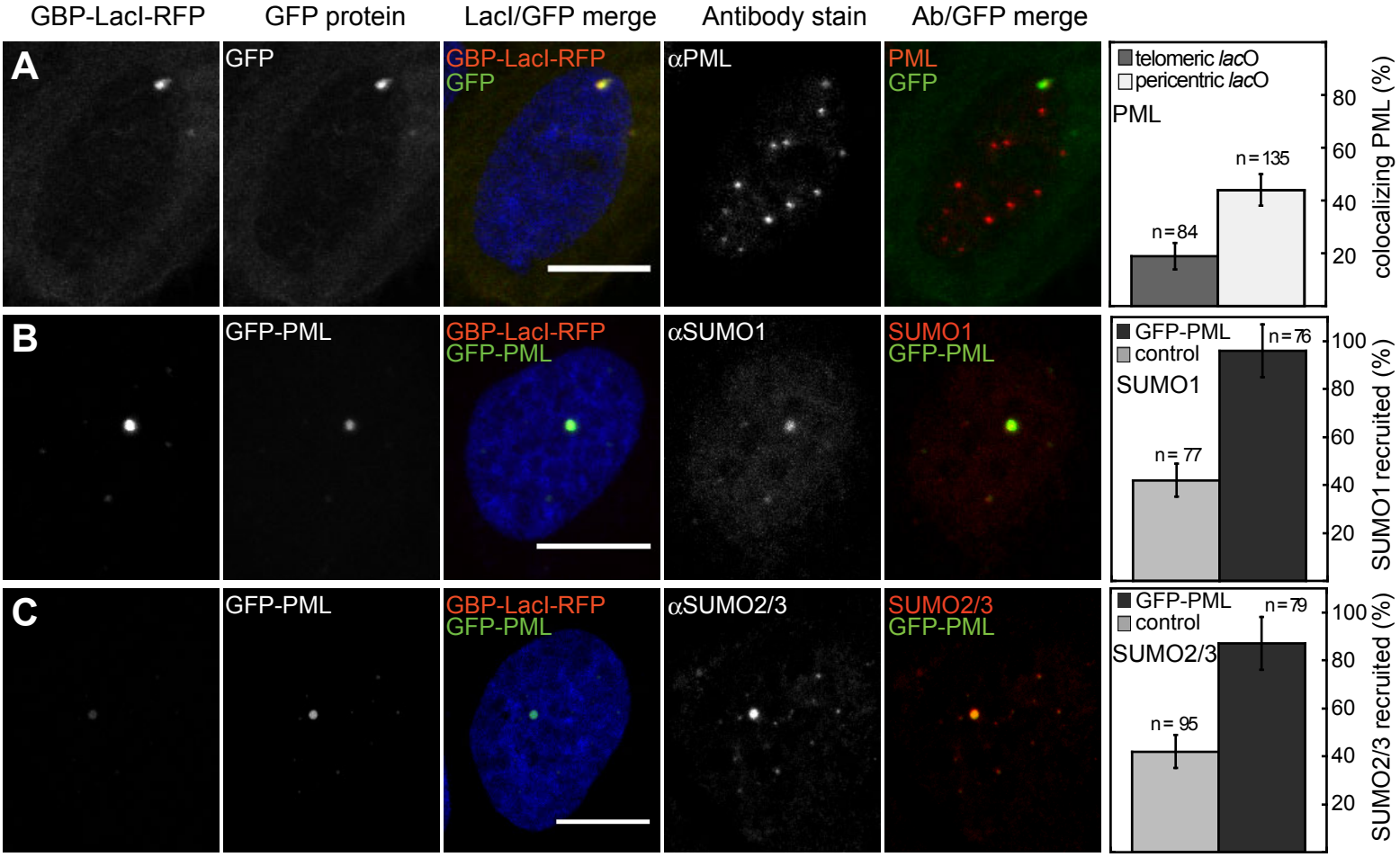
GBP-LacI-RFP
GFP protein
LacI/GFP merge
Antibody stain
Ab/GFP merge
A
GFP
GBP-LacI-RFP
GFP
αPML
PML
GFP
telomeric lacO
pericentric lacO
PML
n=135
n=84
80
60
40
20
colocalizing PML (%)
B
GFP-PML
GBP-LacI-RFP
GFP-PML
αSUMO1
SUMO1
GFP-PML
GFP-PML
control
SUMO1
n=76
n=77
100
80
60
40
20
SUMO1 recruited (%)
C
GFP-PML
GBP-LacI-RFP
GFP-PML
αSUMO2/3
SUMO2/3
GFP-PML
GFP-PML
control
SUMO2/3
n=79
n=95
100
80
60
40
20
SUMO2/3 recruited (%)

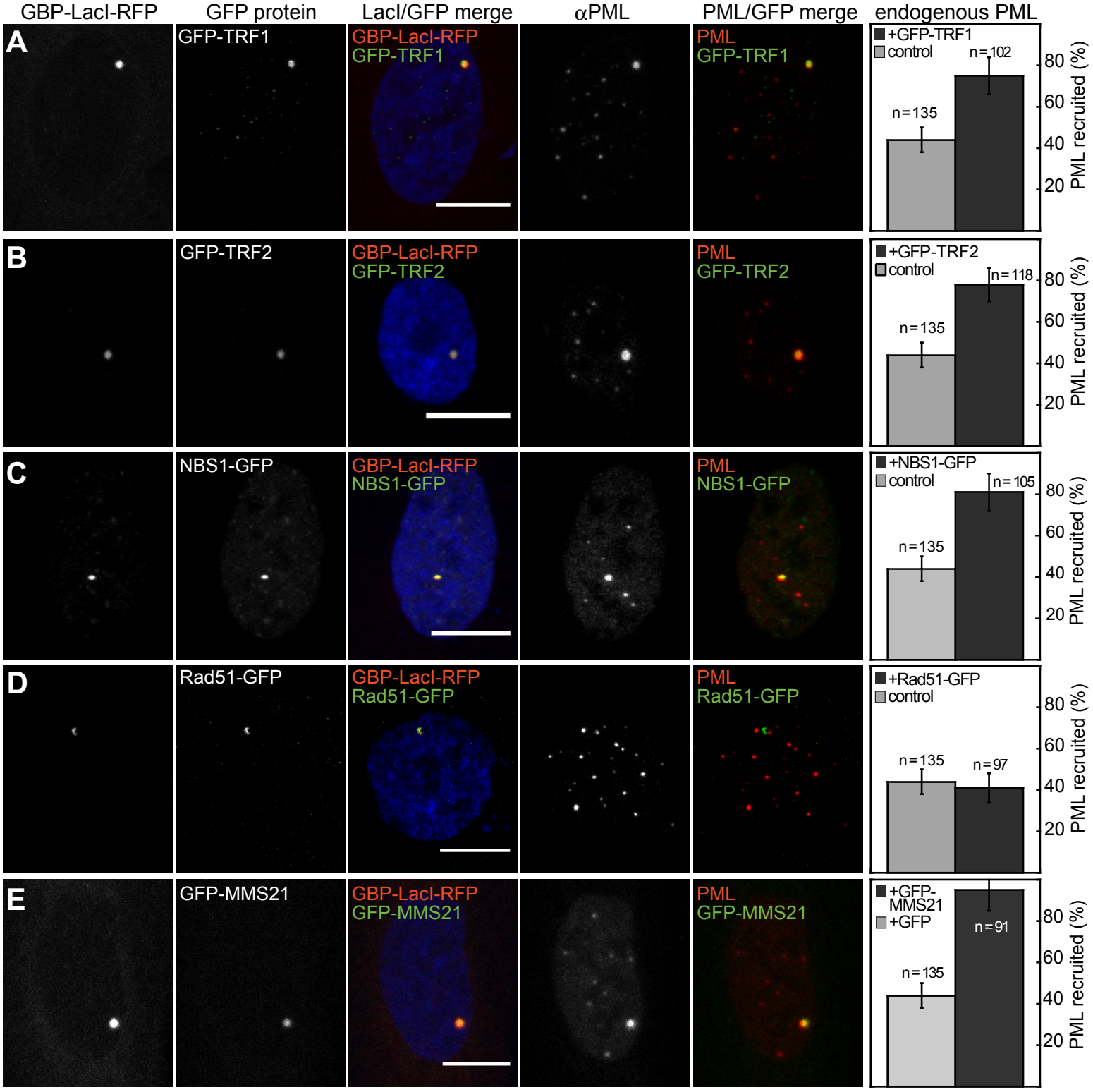
GBP-LacI-RFP
GFP protein
LacI/GFP merge
αPML
PML/GFP merge
endogenous PML
A
GFP-TRF1
GBP-LacI-RFP
GFP-TRF1
PML
GFP-TRF1
+GFP-TRF1
control
n=102
n=135
PML recruited (%)
B
GFP-TRF2
GBP-LacI-RFP
GFP-TRF2
PML
GFP-TRF2
+GFP-TRF2
control
n=118
n=135
PML recruited (%)
C
NBS1-GFP
GBP-LacI-RFP
NBS1-GFP
PML
NBS1-GFP
+NBS1-GFP
control
n=105
n=135
PML recruited (%)
D
Rad51-GFP
GBP-LacI-RFP
Rad51-GFP
PML
Rad51-GFP
+Rad51-GFP
control
n=135
n=97
PML recruited (%)
E
GFP-MMS21
GBP-LacI-RFP
GFP-MMS21
PML
GFP-MMS21
+GFP-
MMS21
+GFP
n=91
n=135
PML recruited (%)
0
20
40
60
80